REPORT DOCUMENTATION PAGE

Form Approved
OMB No. 0704-0188

1. REPORT DATE *(DD-MM-YYYY)*	**2. REPORT TYPE**	**3. DATES COVERED** *(From - To)*
31 March 1954	Final report	

4. TITLE AND SUBTITLE

Electromagnetic Measurements Conducted by the Central Radio Propagation Laboratory During Operation Upshot-Knothole

5a. CONTRACT NUMBER

5b. GRANT NUMBER

5c. PROGRAM ELEMENT NUMBER

6. AUTHOR(S)

5d. PROJECT NUMBER
B/216/E/NBS

5e. TASK NUMBER

5f. WORK UNIT NUMBER

7. PERFORMING ORGANIZATION NAME(S) AND ADDRESS(ES)

National Bureau of Standards, Gaithersburg, MD 20899

8. PERFORMING ORGANIZATION REPORT NUMBER

NBS-3C102

9. SPONSORING / MONITORING AGENCY NAME(S) AND ADDRESS(ES)

Air Force Technical Applications Center, Patrick AFB, FL 32925

10. SPONSOR/MONITOR'S ACRONYM(S)

11. SPONSOR/MONITOR'S REPORT NUMBER(S)

12. DISTRIBUTION / AVAILABILITY STATEMENT

Statement A

13. SUPPLEMENTARY NOTES

Partially declassified version of AD0338549.

14. ABSTRACT

15. SUBJECT TERMS

16. SECURITY CLASSIFICATION OF:			**17. LIMITATION OF ABSTRACT**	**18. NUMBER OF PAGES**	**19a. NAME OF RESPONSIBLE PERSON**
a. REPORT	**b. ABSTRACT**	**c. THIS PAGE**			**19b. TELEPHONE NUMBER** *(include area code)*
U	U	U			

Standard Form 298 (Rev. 8-98)
Prescribed by ANSI Std. Z39.18

#12

~~SECRET~~
~~RESTRICTED DATA~~

AD 338549

DEFENSE DOCUMENTATION CENTER

FOR

SCIENTIFIC AND TECHNICAL INFORMATION

CAMERON STATION, ALEXANDRIA, VIRGINIA

~~RESTRICTED DATA~~
~~SECRET~~

~~RESTRICTED DATA~~

[redacted]

NOTICE: When government or other drawings, specifications or other data are used for any purpose other than in connection with a definitely related government procurement operation, the U. S. Government thereby incurs no responsibility, nor any obligation whatsoever; and the fact that the Government may have formulated, furnished, or in any way supplied the said drawings, specifications, or other data is not to be regarded by implication or otherwise as in any manner licensing the holder or any other person or corporation, or conveying any rights or permission to manufacture, use or sell any patented invention that may in any way be related thereto.

NOTICE:

[redacted]

(5) 603 450

SECRET [redacted]

Copy No. 26

AD No. 338549
DDC FILE COPY

NATIONAL BUREAU OF STANDARDS REPORT

3C102

FINAL REPORT ON
OPERATION UPSHOT-KNOTHOLE
Project No. 8/216/E/NBS

25

Electromagnetic Measurements Conducted by the Central Radio Propagation Laboratory During Operation Upshot-Knothole

By

[redacted]

National Bureau of Standards
Washington 25, D. C.

OSD
5 U.S.C. § 552 (b)(6)

For

Office for Atomic Energy, DCS/O
Department of the Air Force

March 31, 1954

338549

NBS

U. S. DEPARTMENT OF COMMERCE
NATIONAL BUREAU OF STANDARDS

61-11-5814

[redacted]

SECRET

Attch 1

[redacted]

[redacted]

U. S. DEPARTMENT OF COMMERCE
Sinclair Weeks, Secretary

NATIONAL BUREAU OF STANDARDS
A. V. Astin, Director

THE NATIONAL BUREAU OF STANDARDS

The scope of activities of the National Bureau of Standards is suggested in the following listing of the divisions and sections engaged in technical work. In general, each section is engaged in specialized research, development, and engineering in the field indicated by its title. A brief description of the activities, and of the resultant reports and publications, appears on the inside of the back cover of this report.

Electricity. Resistance and Reactance Measurements. Electrical Instruments. Magnetic Measurements. Electrochemistry.

Optics and Metrology. Photometry and Colorimetry. Optical Instruments. Photographic Technology. Length. Engineering Metrology.

Heat and Power. Temperature Measurements. Thermodynamics. Cryogenic Physics. Engines and Lubrication. Engine Fuels. Cryogenic Engineering.

Atomic and Radiation Physics. Spectroscopy. Radiometry. Mass Spectrometry. Solid State Physics. Electron Physics. Atomic Physics. Neutron Measurements. Infrared Spectroscopy. Nuclear Physics. Radioactivity. X-Ray. Betatron. Nucleonic Instrumentation. Radiological Equipment. Atomic Energy Commission Radiation Instruments Branch.

Chemistry. Organic Coatings. Surface Chemistry. Organic Chemistry. Analytical Chemistry. Inorganic Chemistry. Electrodeposition. Gas Chemistry. Physical Chemistry. Thermochemistry. Spectrochemistry. Pure Substances.

Mechanics. Sound. Mechanical Instruments. Fluid Mechanics. Engineering Mechanics. Mass and Scale. Capacity, Density, and Fluid Meters. Combustion Control.

Organic and Fibrous Materials. Rubber. Textiles. Paper. Leather. Testing and Specifications. Polymer Structure. Organic Plastics. Dental Research.

Metallurgy. Thermal Metallurgy. Chemical Metallurgy. Mechanical Metallurgy. Corrosion.

Mineral Products. Porcelain and Pottery. Glass. Refractories. Enameled Metals. Concreting Materials. Constitution and Microstructure.

Building Technology. Structural Engineering. Fire Protection. Heating and Air Conditioning. Floor, Roof, and Wall Coverings. Codes and Specifications.

Applied Mathematics. Numerical Analysis. Computation. Statistical Engineering.

Electronics. Engineering Electronics. Electron Tubes. Electronic Computers. Electronic Instrumentation. Process Technology.

Radio Propagation. Upper Atmosphere Research. Ionospheric Research. Regular Propagation Services. Frequency Utilization Research. Tropospheric Propagation Research. High Frequency Standards. Microwave Standards.

●Office of Basic Instrumentation

●Office of Weights and Measures.

DECLASSIFIED IN FULL
Authority: EO 13526
Chief, Records & Declass Div, WHS
Date: JAN 0 2 2013

(4) NA (5) 603 400

[redacted]

[redacted]

This is a 104 Page Document

NATIONAL BUREAU OF STANDARDS REPORT

(16) NBS PROJECT
1401-40-6822

(17) ~~NBS~~ REPORT
3C102

March 31, 1954

(21) Rept. on (9) FINAL REPORT ON
OPERATION UPSHOT-KNOTHOLE
(16) Project No. 8/216/E/NBS

(6) Electromagnetic Measurements Conducted by the Central Radio Propagation Laboratory During Operation Upshot-Knothole (U).

(7) NA
(8) ...
(11) 31 Mar 54
(12) 101 p.
(13) NA
(14) NA
(15) NA
(17) NA
(18) NBS
(20) SRD
(21) NA

(10) By

[redacted]

National Bureau of Standards
Washington 25, D. C.

OSD
5 U.S.C. § 552 (b)(6)

For

Office for Atomic Energy, DCS/O
Department of the Air Force

NBS

U. S. DEPARTMENT OF COMMERCE
NATIONAL BUREAU OF STANDARDS

[redacted]

[redacted]

[redacted]

~~...ED FROM ...MATIC REGRAD... ...E 5200.10 DOES NOT APP...~~

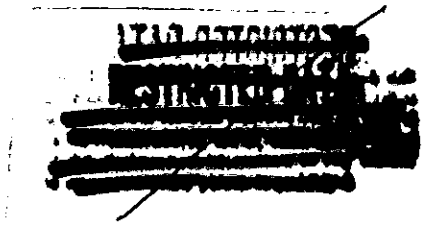

SECRET

SECRET

[redacted]

[redacted]

ABSTRACT

This report describes the electromagnetic measurements conducted by the Central Radio Propagation Laboratory during Operation UPSHOT-KNOTHOLE. Pulse waveforms recorded at the Nevada Proving Ground reveal the original pulse shape before being distorted by the effects of propagation. Records made at distances of one and three thousand kilometers show the changes in waveforms brought about by propagation. Attempts were made to interpret the waveforms received at distant stations in terms of active modes of propagation, and to relate the bomb yield to propagation distance, electromagnetic field strength and energy, detonation height, etc. Expressions are also given relating the attenuation of the pulse to propagation distance.

A

[redacted]

[redacted]

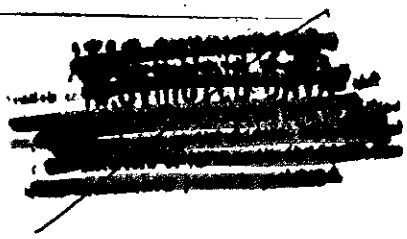

SECRET

[redacted]

ACKNOWLEDGEMENTS

The author wishes to acknowledge the work of members of the Central Radio Propagation Laboratory who have contributed to this project.

Those who performed the tests at the Nevada Proving Ground are: [redacted]

OSD
5 U.S.C. § 552 (b)(6)

Measurements were made at the field stations by: [redacted]

Substantial additions to this report were made by [redacted] in the field of electromagnetic radiation, by [redacted] who performed mathematical analyses, and by [redacted] who generously gave technical advice to this project at critical times.

Special indebtedness must be acknowledged to [redacted] who acted as project adviser and who wrote Chapter IV of this report.

[redacted]

[redacted]

SECRET

SECRET

CONTENTS

[redacted]

[redacted]

[redacted]

[redacted]

[redacted]

[redacted]

[redacted]

ILLUSTRATIONS

[redacted]

[redacted]

[redacted] [redacted]

[redacted]

[redacted]

TABLES

[redacted]

[redacted]

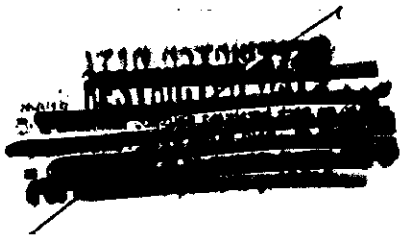

SECRET

SECRET

[redacted]

ELECTROMAGNETIC MEASUREMENTS CONDUCTED BY THE CENTRAL RADIO PROPAGATION LABORATORY DURING OPERATION UPSHOT-KNOTHOLE

by

[redacted]
National Bureau of Standards
Washington 25, D. C.

CHAPTER I

INTRODUCTION

1.1 OBJECTIVE

The objective of this research program is to obtain background information for the development of an automatic, continuously operating electromagnetic surveillance system capable of detecting pulses from atomic weapons detonated in certain suspect areas. A successful electromagnetic detection system would have the advantage of furnishing the earliest and the most accurate detonation times. The true detonation time is of increased importance at times when the atmosphere is already contaminated from a previous explosion. It is thought that a successful detection system can be developed using two or more stations located in low noise areas and utilizing time coincidence recognition. Successful operation would depend upon millisecond timing accuracy and an intimate knowledge of ionospheric propagation conditions along the transmission paths involved.

The Defense Research Laboratory of the University of Texas is concerned with the problems of engineering the detection system, while the Central Radio Propagation Laboratory is primarily concerned with the nature of the generated signal and its modification in form and intensity after propagation by the ionosphere.

[redacted]

[redacted] by law.

[redacted]

[redacted]

1.2 BACKGROUND

The Central Radio Propagation Laboratory conducted radio-frequency detection tests during Operation TUMBLER-SNAPPER using narrow-band equipment at distant sites. These pulses were received following the time of the detonation by approximately the time required for propagation. No strong secondary pulses were received except such as may be attributed to different modes of propagation. However, little information regarding the characteristics of the original pulses could be determined from the results of these measurements. The first successful broadband measurements were made during Operation IVY at distances of 4000 and 8000 km. In order to record the original pulse shapes, it was suggested that future broadband measurements be conducted near enough to ground zero to avoid pulse distortion due to ionospheric propagation.

CHAPTER II

INSTRUMENTATION AND OPERATING PROCEDURE

2.1 OUTLINE OF THE CRPL EXPERIMENTS

Broadband pulses and responses from narrow-band equipment were recorded, together with timing marks, during the UPSHOT-KNOTHOLE tests at the following locations: Nevada Proving Ground; Boulder, Colorado; Ft. Belvoir, near Washington, D. C.; and Stanford, California.

2.1.1 Tests Conducted at the Nevada Proving Ground

The location of the Nevada recording stations was near enough to ground zero to permit recording the waveform before the effects of propagation had appreciably altered its shape, and yet far enough away so that the radiation component of the electromagnetic field predominated over the induction component. A .21-meter vertical probe antenna, mounted on top of a trailer, fed all receivers through a voltage divider and a cathode-follower unit. Equipment having a uniform gain over the frequency range from 1 kc to 2 Mc or higher (3 db point at approximately 8 Mc) was used to record the waveforms. The oscilloscopes were modified to permit self-triggering from either polarity of pulse.

Narrow-band responses from receivers having a 3 Kc bandwidth at half-voltage points and tuned to 2.5 Mc, 10 Mc, and 15 Mc, were recorded on three channels of a four-beam oscilloscope. Timing

[redacted]

[redacted]

marks were recorded on the fourth channel of this oscilloscope. These records provided peak field strength values, at the above mentioned frequencies and bandwidths, as well as the time of reception of the electromagnetic pulse. Detonation times were sent from the Nevada Proving Ground to the distant field stations, and after allowances for propagation delay, positive identification of the desired pulses was possible.

For each event an effort was made to record the broadband wave form on a single record, and also to record the rise time of the initial portions of the pulse on other records, using a more sensitive scale. To accomplish this, five oscilloscopes were used with different gain settings and sweep rates, since the exact relationships between the peak field strength, pulse length, yield, distance from ground zero, tower height, etc., were not known. Reliable records of waveforms were obtained for all events except No. 1, in which case the signal exceeded the dynamic range of the equipment. As experience was gained in predicting the strength of the signal, other records of interest were obtained using higher gains, faster sweep rates, and longer delay lines. By these means, the small amplitude detail that preceded the main negative pulse was revealed.

Additional experiments were conducted for Shots No. 1, 2, 3, and 4 to gain information regarding the relative strength of the horizontally and vertically polarized components of the radiation field. This was accomplished by recording the horizontally-polarized component of the downcoming sky wave after ionospheric reflection. This component is related in amplitude to the horizontally-polarized component radiated by the source.

2.1.2 Tests Conducted at Boulder, Colorado; Washington, D. C; and Stanford, California

At Boulder and Washington vertical antennas were used with cathode-follower units which were connected by coaxial cables to the broadband equipment and the narrow-band receivers. The bandwidth of the broadband equipment used at these stations was sufficient to record the waveforms with considerable fidelity. However, at Washington it was necessary to use a filter to reject station NSS for Shots No. 1 through 8.

The pulse outputs of the three narrow-band receivers, which were tuned to frequencies of 15 kc, 30 kc, and a channel near the maximum usable frequency for the path, were recorded on three channels of a four-beam oscilloscope. The fourth channel was used to record timing marks. The detonation times determined from the Nevada

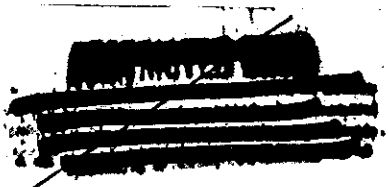

measurements, with allowances for propagation delay, were used to positively identify the pulses recorded at the distant stations. The use of these times was the only means of identification on occasions when the atmospheric noise level was unusually high, when the bomb was very small, or when propagation conditions were unfavorable.

Equivalent peak field strengths at frequencies of 15 and 30 kc were obtained from the narrow-band measurements.

The broadband waveforms recorded at the distant stations were used to obtain the frequency distributions of the energy of the pulses. The effect of ionospheric propagation upon the pulses can be determined by comparing the frequency functions of the waveforms recorded at the Nevada sites with those recorded at the distant field stations. The bandwidth required for faithful pulse reproduction decreases with increasing distance, since the effect produced by the ionosphere is similar to that produced by a low-pass filter. For this reason the bandwidth of the broadband equipment necessary at distances of 20 km extended from 1 kc to 2 Mc, while the bandwidth of the equipment used at 1000 and 3000 km extended from about 1 to 80 kc.

Measurements at very low frequencies were made at Stanford University by members of the University staff under a subcontract with the Central Radio Propagation Laboratory. The loop antenna and amplifier system, which had been designed and used previously for the reception of atmospherics at low levels, were used. The gain of the system was very high, and the bandwidth extended from about 500 cps to nearly 200 kc. For most shots, the time of occurrence, the waveform of the signal, and the peak amplitude were recorded, the latter being expressed in terms of antenna voltage.

2.2 DESCRIPTION OF TIMING METHOD USED AT ALL STATIONS

The same instrumentation for obtaining the time of reception of the electromagnetic pulses was used at all stations. A 100 kc secondary frequency standard was used, together with frequency dividers, to give 25 cps output. The 25 cps output was then twice divided by five to obtain one pulse per second. A mechanical arrangement was used to permit the 59th second mark to be omitted. The timer was operated in the following manner: First the 100 kc secondary frequency standard was adjusted so that one of the harmonics was as nearly as possible synchronized with the highest frequency signal recordable from station WWV (or WWVH). The divider units were checked to be sure they were in synchronism with the 100 kc secondary frequency standard and dividing

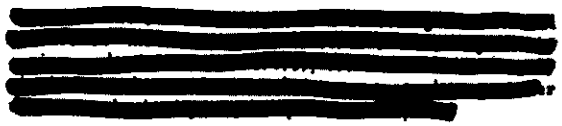

properly. The once-per-second pulse output of the timer unit was then synchronized with the seconds ticks received from station WWV. The audio output of a receiver tuned to station WWV was connected to the vertical deflection plates of an oscilloscope, and the seconds pulses from the timing unit were allowed to trigger the sweep of this oscilloscope. A phase-shifting circuit in one stage of the frequency divider was then adjusted until the seconds ticks from WWV, which consist of five cycles of 1000 cps, were seen on the oscilloscope. The two units were in synchronism when the start of the oscilloscope sweep coincided with the very beginning of each WWV seconds tick. Figure 3.64 is a photograph of a time comparison between seconds marks received from WWV and the timer unit. Note that the timing unit pulse in this figure is about 1.6 milliseconds later than the beginning of the seconds mark received from WWV.

2.3 DESCRIPTION OF EQUIPMENT USED AT THE NEVADA PROVING GROUND

The equipment used in Nevada was divided among three sites with only two sites in operation simultaneously. At Site 7.1A were located the broadband equipment, timing equipment, and narrow-band receivers. The other two sites, 7.1B and 7.1C, were used only for broadband measurements. Power was supplied by portable diesel generators at all three sites. Figure 2.1 is a block diagram of the equipment arrangement as used at the main site.

2.3.1 Antenna Systems and Cathode-Follower Units

Various antennas and cathode-follower arrangements were tried during the first three shots at the main site. For Shot No. 1, the field strength exceeded the dynamic range of the equipment. For Shot No. 2 a 7.19-meter vertical antenna, with a .38-meter diameter aluminium disk on top, was used at the main site. It was thought that this disk would improve the low-frequency response, but later it was found to be unnecessary, and it was not used after Shot No. 3. A schematic diagram of the cathode-follower unit used for Shot No. 2 is shown in Figure 2.2.

At the main site the base of the antenna was connected directly to the cathode-follower grid for Shot No. 3. For Shots No. 4 through 11 a capacity divider was included in the cathode follower to decrease the voltage delivered by the antenna to the cathode-follower unit. The voltage divider consisted of an additional capacitor of 47 μμfd connected to ground and acting with the antenna base capacity of 10.7 μμfd. The input impedance of the cathode-follower unit was very high, so that over the frequency range of interest, the open circuit voltage of the antenna was impressed upon the recording equipment.

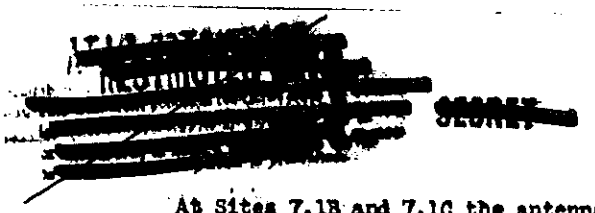

At Sites 7.1B and 7.1C the antennas used for Shots No. 3 through 11 were identical to that used at Site 7.1A, except that their bases were connected directly to the oscilloscope probes. The probes, which had an input impedance of 10 megohms shunted by an input capacity of 13 μμfd, provided a voltage attenuation of 10:1. To obtain amplitude calibrations, a voltage from a standard signal generator was applied to the input of the cathode-follower unit through a capacitor representing the antenna.

2.3.2 Narrow-band Measurements

Three Hammarlund SP-600 receivers, using the 3 kc bandwidth position, were tuned to frequencies of 2.5, 5 and 15 Mc. The signal voltages were applied to the receivers from the cathode-follower unit. The radio-frequency gain controls were set by estimate and no automatic volume control was used. The outputs from the receivers were taken from the intermediate frequency output and detected using a 1N34 crystal, a 10,000 ohm resistor, and a 0.001 μfd capacitor. These voltages were applied to the horizontal deflection plates of a four-beam oscilloscope. The fourth channel of this oscilloscope was used to record timing marks as previously described (Fig. 3.33). Photographic records were made using an NBS strip film camera which moved the film vertically past the face of the oscilloscope at the rate of 17 inches per second.

2.3.3 Broadband Measurements

At the main site five Tektronix type 513-D oscilloscopes were used with different sensitivities and sweep speeds. They were modified to trigger either from positive or negative signals. When external triggering was used, the trigger voltage was obtained from a separate 1.83-meter antenna, which permitted the earliest aspects of the pulse to be recorded. The signal voltage was normally delayed 0.25 μsec with respect to the start of the sweep. The sweep delay time was increased to 0.4 μsec by adding an external delay line.

Amplitude calibrations were accomplished by applying a voltage, through a dummy antenna, to the input of the cathode follower from a standard signal generator and measuring the corresponding deflections produced on the oscilloscopes. The broadband equipment had linear amplitude response up to 4 cm of oscilloscope deflection.

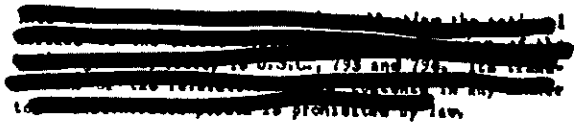

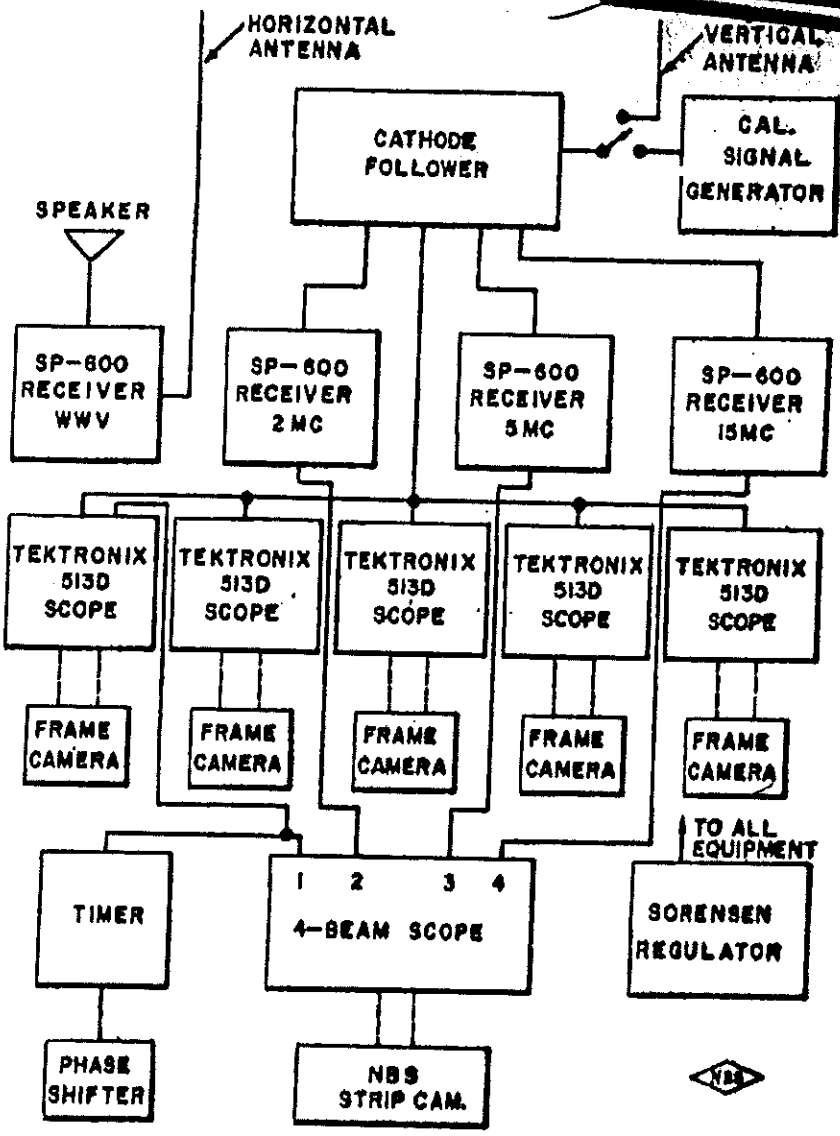

FIG. 2.1 BLOCK DIAGRAM OF EQUIPMENT USED AT THE NEVADA PROVING GROUND (MAIN SITE)

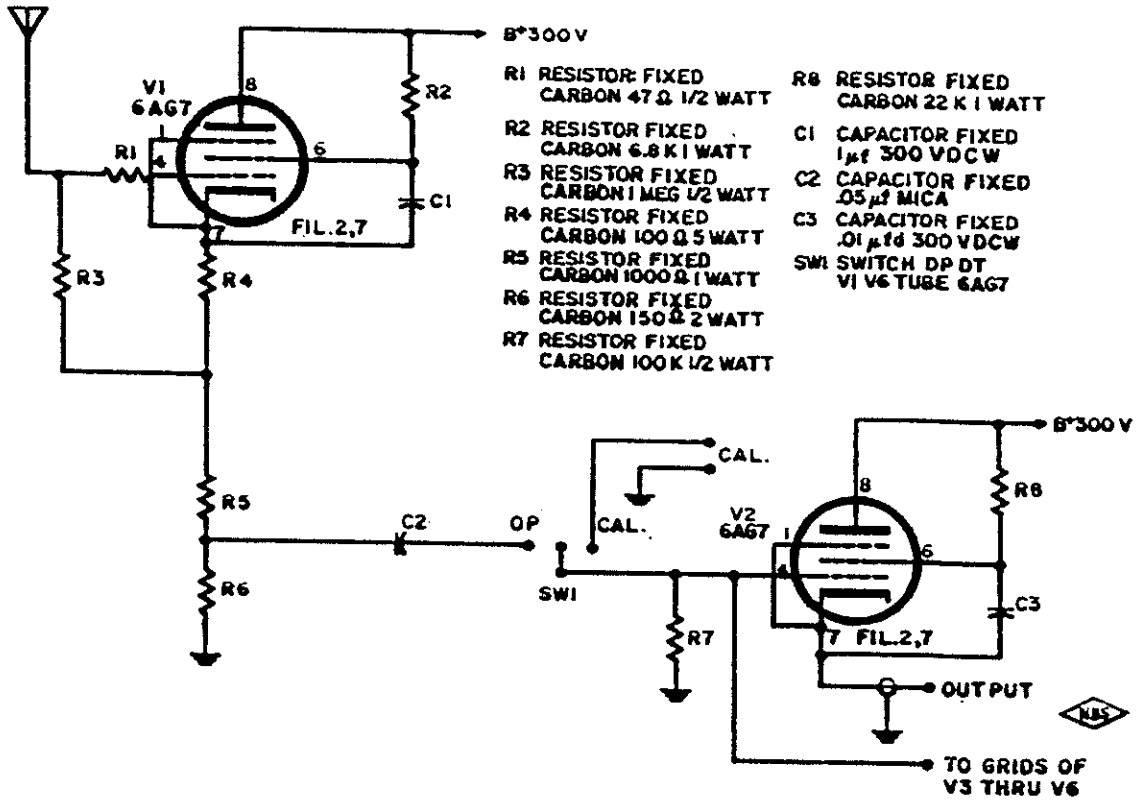

FIG. 2.2 CATHODE FOLLOWER UNIT USED AT THE NEVADA PROVING GROUND (MAIN SITE) FOR SHOT NO. 2

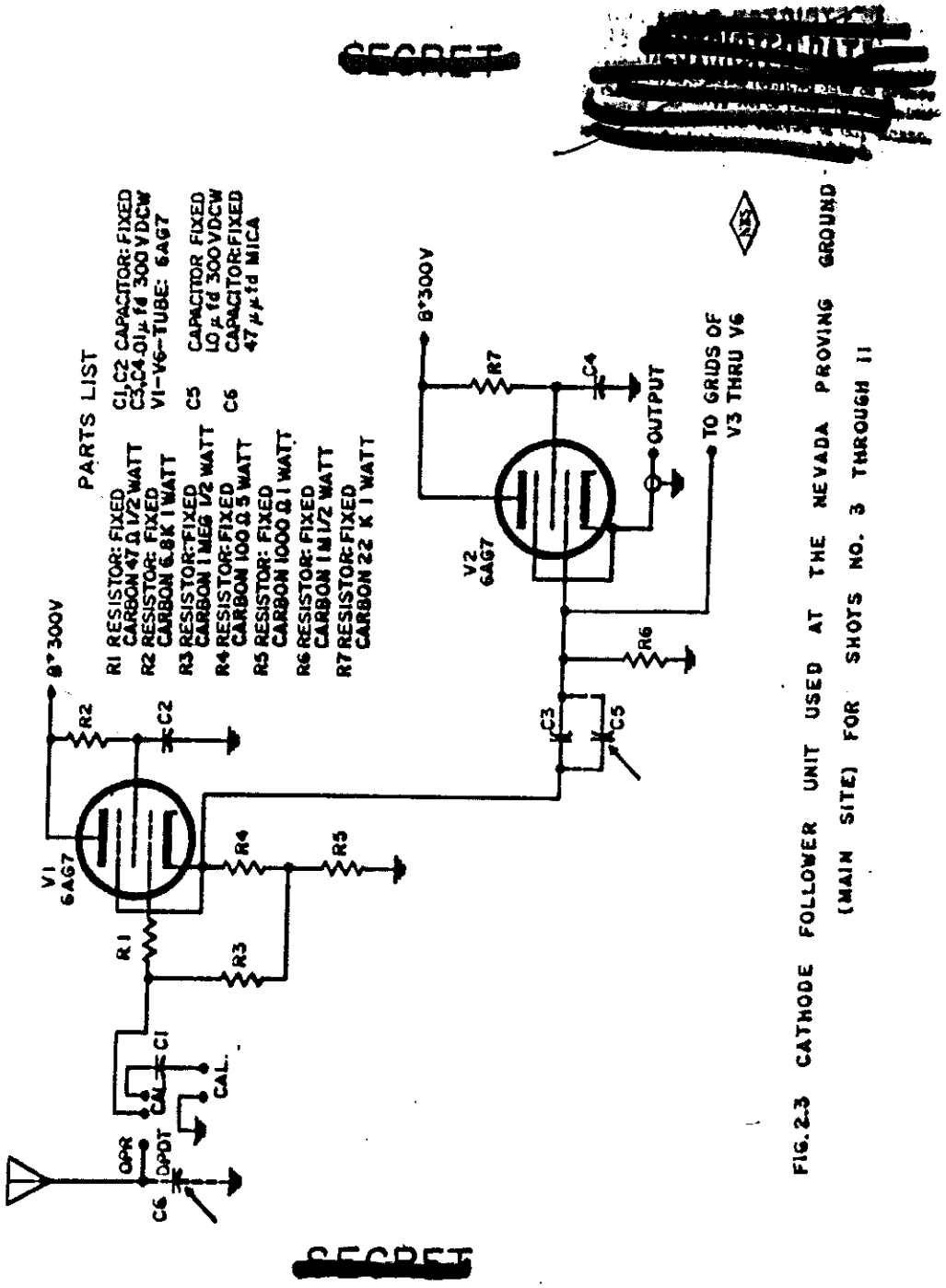

FIG. 2.3 CATHODE FOLLOWER UNIT USED AT THE NEVADA PROVING GROUND (MAIN SITE) FOR SHOTS NO. 3 THROUGH 11

[redacted]

[redacted] calibrations were made on each oscilloscope to determine the degrees of skewness that existed between the grid lines on the face of the cathode ray tube and the directions, horizontal and vertical, in which the spot was deflected. Photographic records were made of vertical skewness for each of the eight horizontal centimeter marks and horizontal skewness over the vertical range of four centimeters for each oscilloscope. These values of skewness were taken into consideration when computing the frequency functions from the waveforms.

The frequency response for each of the broadband receivers used at the main site was obtained by feeding a signal into the cathode follower and measuring the corresponding deflection produced on each of the oscilloscopes at different frequencies ranging from 1 kc to 30 Mc. The results are shown in Figure 2.4. It can be seen from this figure that in all cases the response was uniform at least from 1 kc to 2 Mc and slowly diminished at higher frequencies.

The transient response of the broadband equipment was determined by feeding a square wave into the broadband system and observing the rise time on the oscilloscopes. Using a 0.26-μsec square-wave input to the cathode follower, a rise time of 0.02 μsec was obtained. Photographs of the transient response of the equipment are shown in Figure 2.5. No ringing or overshoot is observed at any pulse length. The fastest rise time observed for the electromagnetic pulses from detonations was of the order of 0.2 or 0.3 μsec, while the rise time for the equipment was .02 μsec.

Broadband deflections were converted into equivalent values of vertically-polarized field strengths by matching the peak deflections with a sinusoidal voltage from the standard signal generator. The peak value of voltage required to match the deflection and the antenna effective height in meters were used to obtain field strength in units of volts per meter.

The antenna used for Shot No. 1 had a physical length of 0.43 meters. Its effective height was determined in the following manner. A field-strength meter was set up at a point about 200 feet away from the main site. The assumption was made that the field strength at the main site and at the field strength meter was the same value. The measurements demonstrated that the magnetic vectors received from distant VLF stations were of the same magnitude on top of the trailer and at the point 200 feet away. One of the narrow-band receivers was tuned to the same distant station as the field-strength meter. Radio-range stations, NSS and NPM were used for calibration.

[redacted]

[redacted]

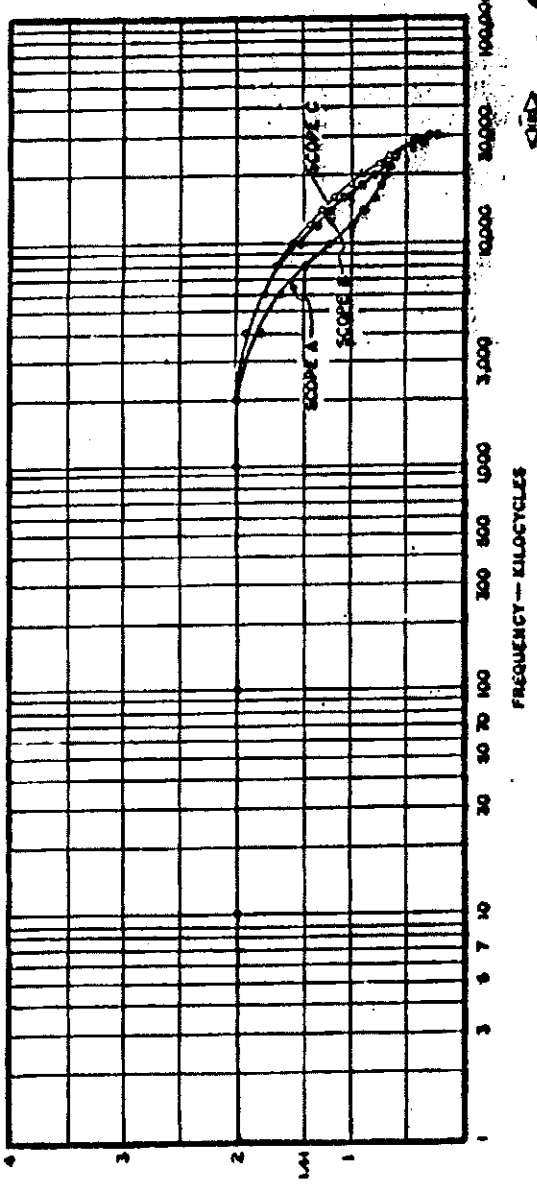

FIG 2.4 AMPLITUDE VS FREQUENCY RESPONSE OF BROADBAND EQUIPMENT USED AT THE NEVADA PROVING GROUND (MAIN SITE)

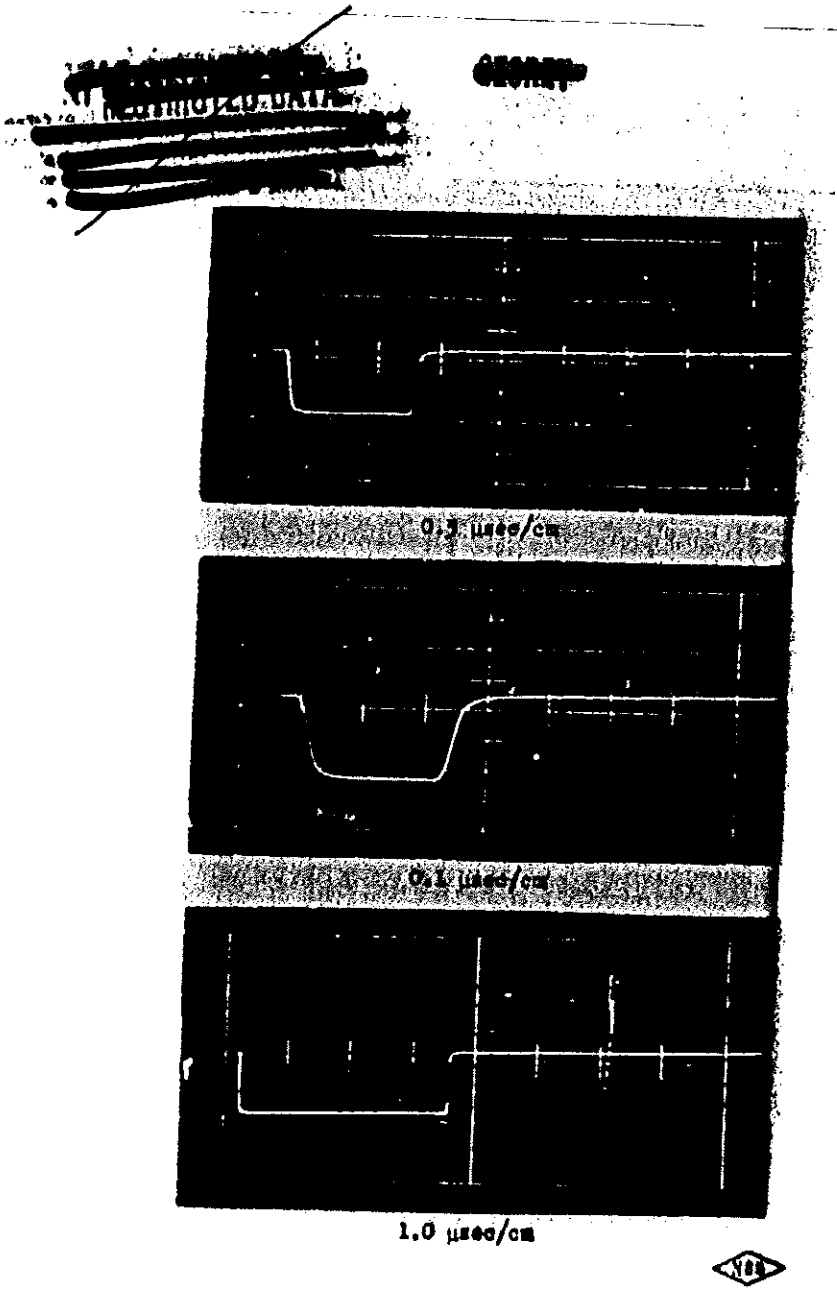

Fig. 2.5 TRANSIENT RESPONSE OF NEVADA PROVING GROUND EQUIPMENT

The receiver output voltage and the value of field strength measured with the field-strength meter were noted. The antenna under calibration was then disconnected, and the signal generator was connected to the input of the cathode-follower unit through a capacitor representing the antenna. The peak value of signal-generator voltage necessary to match the peak receiver deflection was noted. The ratio of peak signal-generator voltage thus obtained to the value of measured peak field strength gave a value of effective height of 0.1 meters for the 0.43-meter antenna.

Using formulas by King and Blake[1], accurate values of input self-resistance and self-reactance of a symmetrical antenna, based on Hallen's analysis, were calculated. These formulas give a much better approximation than those derived, assuming a sinusoidal distribution of current. For the 0.43-meter antenna the effective height was calculated to be 0.12 meters.

The values of effective height of the short antennas used at the Nevada Proving Ground are considerably less than those obtained using one-half of the physical length of the antennas. These differences arise from the fact that the antennas employed here are not sufficiently short, in terms of their capacitance effect to ground, to justify the linear current distribution which results in the value of effective height equal to one-half the physical length.

For Shot No. 2 a .19-meter vertical antenna, top-loaded with a .38-meter diameter disk, was used. The top loading served to increase the effective height over that of a plain .19-meter vertical antenna. An effective height of 0.10 meters was calculated for this antenna, assuming a linear current distribution produced by the top loading.

For Shots No. 3 through 11 a .21-meter antenna, followed by suitable capacity voltage dividers, was used to record the waveforms. Due to the low pick-up factor of this short antenna, it was difficult to measure its effective height by receiving distant, very low frequency stations. However, the values of antenna capacity (3.15 μμfd) and antenna base capacity (8.25 μμfd) were determined in the field using the substitution method. Again, using formulas by King and Blake[1] the antenna capacity was calculated to be 3.60 μμfd, compared to the measured value of 3.15 μμfd. The effective height was calculated to be .07 meters.

[redacted]

In calculating the values of field strength and energy for Shots No.2 an effective height value of 0.1 meters was used; for Shots No. 3 through 11, an effective height value of 0.07 meters was used. These values are appropriate in the very low frequency region and at these short ranges where the surface wave predominates. At higher frequencies, about 1 Mc or so, where the direct and ground-reflected components predominate, the actual height above the ground of the .21-meter antenna cannot be neglected. The antenna effective height was determined at frequencies between 3 and 25 Mc, using a target transmitter furnished by the Sandia Corporation. The results of these measurements suggest a value of effective height of 0.24 meters and illustrate the dependence of antenna gain upon height at these frequencies.

2.3.4 Vertical Incidence Ionospheric Measurements

An additional experiment was arranged in an attempt to determine whether appreciable horizontally-polarized energy was radiated by the source. A loop antenna, having eleven turns and which was .78 meters in diameter, was mounted on a tripod so that its center was about 6 feet above the earth. The loop was placed in the vertical plane and oriented so that minimum energy would be received directly from the source. The oscilloscope sweep time was long to permit receiving any possible ionospheric reflections. It was reasoned that a signal recorded from the ionospheric layers must have been originally horizontally polarized. This assumes that the original polarization is preserved after ionospheric reflection. One side of the loop antenna was grounded, and it was damped with a resistance to prevent ringing. A Tektronix type 121 preamplifier was used at the terminals of the loop antenna, and a 200-foot length of coaxial cable connected the output of the preamplifier to the recording oscilloscope at the main site.

In order to calibrate the system, a low impedance signal generator was inserted in series with the loop antenna. The effective height of the antenna was calculated by using the expression:[2]

$$\frac{E}{e} = \frac{2\pi NA}{\lambda}$$

[redacted]

where

E = resultant voltage acting around the loop
e = field intensity of signal at the loop in volts per meter
N = number of turns in loop = 11
λ = wavelength of signal in meters
A = area of loop in square meters

At a frequency of 16 kc, $\frac{E}{e}$ = 1.7 meters.

2.4 DESCRIPTION OF INSTRUMENTATION USED AT BOULDER, COLORADO

This test site which was seven miles east of Boulder, Colorado, had a low noise level. The great-circle distance between the Nevada test site and the Boulder site is 1005 km.

For the broadband waveform measurements, one output of the cathode-follower unit went to the oscilloscope through a bandpass filter designed to reduce 60 cps pickup and interference from radio range and local broadcasting stations. The oscilloscope was modified to permit self-triggering with either polarity of incoming signal. The broadband pulses were recorded from the oscilloscope using a 35 mm camera with a film speed of 10 inches per second.

Other outputs of the cathode-follower unit went to the narrow-band, low-frequency receivers having bandwidths of about 422 cps. These receivers were tuned to frequencies of 15 and 30 kc. A receiver with a bandwidth of 3 kc was tuned to a channel near the maximum usable frequency for the path. The pulses from the three receivers, together with timing marks, were recorded from a four-channel oscilloscope, using a 35 mm camera, with a film speed of 17 inches per second. Trigger gate pulses from the broadband oscilloscope were mixed with the timing marks, so that the times when broadband waveforms were recorded could be determined. A four-channel oscilloscope record from Boulder is shown in Figure 3.75.

In calibrating the narrow-band equipment, the output of a Navy type LP-5 signal generator was fed through a dummy antenna to the input of the cathode-follower unit. The rms output of the signal generator necessary to match the peak deflection recorded during the

[redacted]

[redacted] SECRET

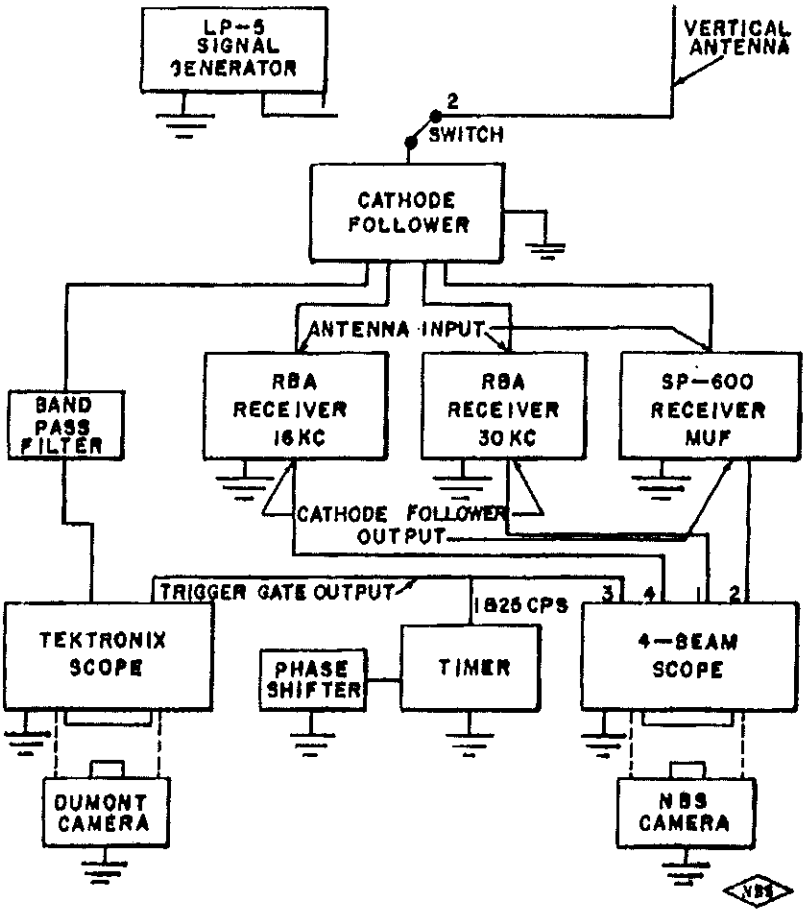

FIG. 2.6 BLOCK DIAGRAM OF EQUIPMENT USED AT BOULDER, COLO.

SECRET

[redacted]

detection test was obtained. Peak voltages corresponding to the rms calibration voltages were divided by the appropriate values of antenna effective height to convert to peak values of vertically-polarized electric field.

Since the reciprocal of the receiver bandwidth (2.3 msec) is much greater than the duration of the received impulses (about 0.5 msec), the receiver output response is practically independent of the shape of the impulse and is determined by its area. Jansky[3] confirmed that the peak output voltage is proportional to bandwidth, for bandwidths less than about 20 kc.

After the test series was over, it was found that the 15-kc receiver used at Boulder had previously been modified for another application. The same modifications were made on an RBA receiver in the Washington laboratory, and the bandwidth was found to be 630 cps. Without the modifications, the bandwidth was 420 cps. Because the 15-kc measurements made at Boulder are considered to be unreliable, the data are not presented.

Amplitude calibration of the broadband equipment was made by connecting the standard signal generator to the input of the cathode-follower unit and obtaining the rms output necessary to produce one centimeter peak-to-peak deflection on the oscilloscope. This sensitivity calibration was made at only one frequency, since the equipment, from cathode follower to the output of the oscilloscope, has a flat response over the bandwidth used. However, due to the loading effect by the equipment on the antenna, at the lowest frequencies, the response of the installation was 3 db down at a frequency of 12 kc.

Two different methods were used to obtain the values of antenna effective height, and the results of these two methods are in fair agreement. It is thought that nearby overhead power lines were responsible for the inconsistent results obtained in measurements of field strengths from distant, very low frequency stations.

The antenna at Boulder was 31.5 feet long, the bottom end of which was 8 feet above the earth. A 6-foot horizontal lead-in wire, also 8 feet above the earth, was connected to the cathode-follower unit. An 8-foot wire extended from the cathode follower to a ground stake. This antenna was considered to be 40 feet (12 meters) long, with its base at the ground. Using formulas by King and Blake[1] the

[redacted]

[redacted] SECRET

effective height of the antenna (for the open circuit case) was calculated to be 3.7 meters. Unfortunately, the equipment loaded the antenna. The equivalent circuit of the antenna and the input circuit to the cathode follower are shown in Figure 2.7. The circuit values were obtained from radio-frequency bridge measurements.

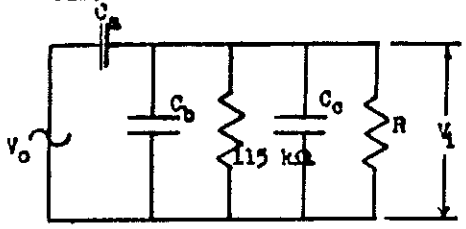

Antenna Equivalent Circuit
Boulder, Colorado

Figure 2.7

C_a = antenna capacity, 72 μμfd

C_b = antenna base capacity, 15 μμfd

C_c = input capacity to cathode-follower unit, 30 μμfd

R = input resistance to cathode-follower unit, 780,000 ohms

The ratios of open-circuit antenna voltages to voltages supplied to the input of the cathode-follower unit, V_o/V_i, were calculated at a series of frequencies. The values of antenna effective height realized at frequencies between 5 and 30 kc are the product of the theoretical effective height of 3.7 meters and the appropriate values of V_o/V_i as shown in Table 2.1.

TABLE 2.1

CORRECTED EFFECTIVE HEIGHT OF ANTENNA AT BOULDER

f(kc)	V_o/V_i	Effective Height (meters)
5	0.24	3.7 x 0.24 = 0.88
10	0.40	3.7 x 0.40 = 1.5
15	0.48	3.7 x 0.48 = 1.8
30	0.57	3.7 x 0.57 = 2.1

[redacted]

Since the peak in energy occurred at frequencies near 16 kc, the corresponding effective height of 1.8 meters was used in calculating the values of energy recorded at Boulder. Although this is not exact, it is a good approximation, since the effective height is less than 1.8 meters at frequencies below 16 kc and greater than 1.8 meters at frequencies above 16 kc.

The equivalent values of field strength recorded at different frequencies were calculated by dividing the peak-to-peak voltage deflections, obtained on the oscilloscope, by the proper values of antenna effective height.

2.5 DESCRIPTION OF INSTRUMENTATION USED AT WASHINGTON, D. C.

The recording site was located at the CRPL Field Station at Ft. Belvoir, Virginia, twelve miles south of Washington, D. C. This is at a great-circle distance of 3400 km from the Nevada Proving Ground.

The arrangement of the recording equipment is shown in the block diagram of Figure 2.8. The vertical antenna was 21 feet long, with the bottom end about 3 feet above the earth. It was located 50 feet from the recording building and connected to a cathode-follower unit directly at its base. Coaxial cables were run from the cathode-follower unit to the equipment inside the building.

For the broadband measurements, a Tektronix type 121 preamplifier, a filter unit, and a Tektronix 513-D oscilloscope were used. The oscilloscope was modified to trigger on either polarity of incoming signal. The waveforms were recorded from the oscilloscope using a 35 mm camera and a film speed of 10 inches per second.

U. S. Navy type RBA receivers, having a bandwidth between 3 db points of about 420 cps, were used to record pulses at frequencies of 15 and 30 kc. A high-frequency receiver, with a bandwidth of about 3 kc, was tuned to a channel near the maximum usable frequency for the path. The pulses from the three receivers, together with timing marks, were recorded from a four-channel oscilloscope using a 35 mm strip camera, and a film speed of 17 inches per second. Trigger gate pulses from the Tektronix oscilloscope were mixed with the timing marks so that it was possible to identify the exact times when broadband pulses were recorded.

[redacted]

SECRET

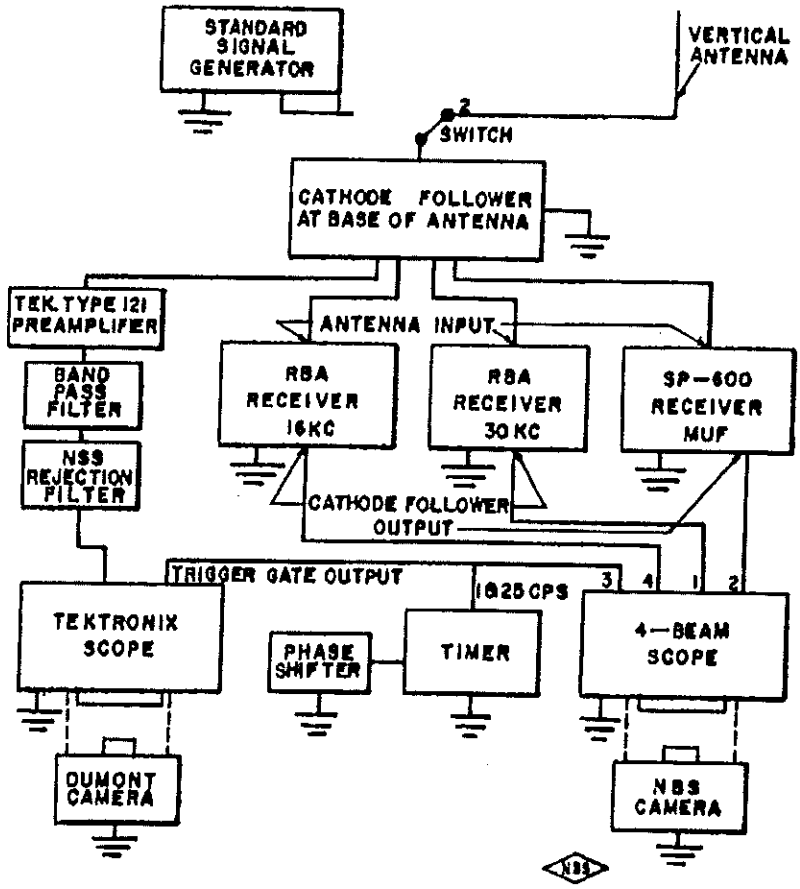

FIG. 2.8 BLOCK DIAGRAM OF EQUIPMENT USED AT FT. BELVOIR, VA NEAR WASHINGTON, D. C.

SECRET

In calibrating the narrow-band equipment the signal-generator output was connected to the input of the cathode-follower unit located at the base of the antenna. The voltage outputs of the signal generator required to match the peak deflections recorded during the detection tests were used with appropriate values of antenna effective height to obtain equivalent values of vertically polarized electric field.

The filter unit which was used in the broadband equipment was designed to reduce 60 cps pickup and to provide a gradual cutoff at frequencies above 100 kc so as to reduce interference from broadcast stations. For Shots No. 1 through 8 it was necessary to use an additional filter in the broadband equipment to reject station NSS at a frequency of 18 kc. This station, which is located at Annapolis, Maryland, only 30 miles away, produced severe interference. Since the peak in energy occurred at frequencies near 15 kc, the necessity of using the NSS rejection filter was most unfortunate. An arrangement was finally made with the Navy which resulted in NSS being off the air for Shots No. 9, 10 and 11. Thus, the NSS rejection filter was not used for these events.

Two methods were used to determine the effective height of the antenna. By measurement, the effective height at a frequency of 16 kc was found to be 2.9 meters. Using formulas by King and Blake[1], a value of 2.1 meters was calculated.

The equivalent circuit of the antenna and input circuit to the cathode-follower unit is shown in Figure 2.9. The circuit values were obtained from radio-frequency bridge measurements.

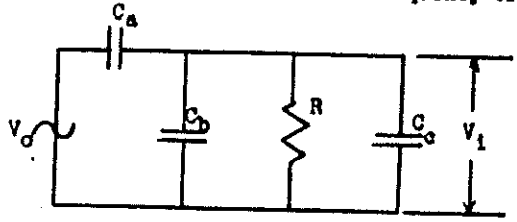

Antenna Equivalent Circuit
Washington, D. C.
Figure 2.9

C_a = antenna capacity, 65 μμfd

C_b = antenna base capacity, 5 μμfd

C_c = input capacity of cathode-follower unit, 30 μμfd

R = input resistance to cathode-follower unit, 780,000 ohms

The ratios of open circuit antenna voltage to voltage supplied to the input of the cathode-follower unit, V_o/V_i, were calculated at a series of frequencies. The value of antenna effective height used in this report, which is the product of the antenna effective height for the unloaded case and the appropriate value of V_o/V_i, is 1.4 meters.

TABLE 2.2

CORRECTED EFFECTIVE HEIGHT OF ANTENNA AT FT. BELVOIR

f(kc)	V_o/V_i	Effective Height (meters)
5	0.62	0.62 x 2.1 = 1.3
10	0.66	0.66 x 2.1 = 1.4
15	0.67	0.67 x 2.1 = 1.4
30	0.67	0.67 x 2.1 = 1.4
100	0.68	0.68 x 2.1 = 1.4

The above results indicate that the overall response of the broadband equipment, including the antenna but without the NSS filter, is flat within 1 db from 5 kc to 100 kc.

SECRET

[redacted]

SECRET

[redacted] SECRET

CHAPTER III

DISCUSSION OF PHOTOGRAPHS

3.1 GENERAL

The photographs recorded at the Nevada Proving Ground are not grouped according to shot sequence in this report. Photographs of some of the pulses recorded at the Nevada Proving Ground and their corresponding frequency functions have been arranged on adjacent pages so that they may be viewed at the same time. Additional records for each shot are presented on the pages following the presentation of frequency functions obtained at the Nevada Proving Ground. The frequency functions were computed by Fourier analysis from the recorded pulses and are plotted in percent of maximum amplitude as a function of frequency.

The pulses were photographed through a centimeter grid, but all of the photographs have not been reproduced to original size. When scaling values of amplitude and time from these records, the grid lines on each figure should be considered as being 1 centimeter apart.

The great-circle propagation distance from the Nevada Proving Ground to Boulder, Colorado, is 1000 km, and all of the records recorded at Boulder have the caption "1000 km from ground zero". The records made at Ft. Belvoir, Virginia, near Washington, D.C. are labeled "3400 km from ground zero".

Occasionally it will be noted that the leading edges of the pulses recorded on the four-channel records are not in alignment. This condition occurred because the spots of the four-beam oscilloscopes were purposely staggered to prevent overlapping of the narrow-band responses and does not imply any lack of simultaneity in recording the different aspects of the phenomena.

3.1.1 Discussion of Photographs from the Nevada Proving Ground

Shot No. 1

In preparation for this test the value of antenna effective height was estimated, and the expected value of field strength was calculated using the following expression which was suggested by members of the Los Alamos Scientific Laboratory.

[redacted] SECRET

[redacted]

$$E = \frac{120\sqrt{Y}}{d} = \frac{120\sqrt{16}}{9.1} = 50 \text{ v/m}$$

where

Y = bomb yield in kilotons = 16
d = distance in miles = 9.1
E = field strength (volts/meter) = 50 v/m

This empirical relation was determined from data recorded during Operation IVY but had not been tested for bombs of smaller size. The gain of the recording equipment was adjusted to permit recording a field strength of 50 v/m, and a sweep rate of 250 μsec/cm was used. As seen in Figure 3.9, the data is of limited use because the dynamic range of the recording equipment was exceeded, and the sweep rate was too slow.

DOE Section 6.2(a) OSD Section 6.2 (a)

Shot No. 2

Shot No. 2, which was a 24-kiloton weapon, was detonated on top of a 300-foot tower. [redacted] The same pulse, recorded with a 50 μsec/cm sweep rate, is shown in Figure 3.24, and with a 1 μsec/cm sweep rate in Figure 3.25. The latter shows the rise time of the first negative pulse. Figure 3.26 is a record of sky-wave reflections obtained using broadband equipment and a slow sweep rate. The first envelope corresponds to the energy received directly from the source. The first sky-wave reflection, which has a relatively small amplitude, occurs at about 550 μsec, corresponding to a virtual height of reflection of about 83 km. This experiment is discussed later in this report.

Shot No. 3

Figure 3.3 shows the pulse recorded from a 0.21-kiloton weapon, detonated on top of a 300-foot tower. The peak amplitude is about 125 v/m. The corresponding frequency function, Figure 3.3

[redacted]

[redacted] SECRET

reveals that although the energy peaks at a frequency near 35 kc, the peak is not nearly as sharp as that for Shot No. 2. A fast sweep presentation, Figure 3.27, reveals the rise time and duration of about 5.5 μsec of the negative pulse. The same pulse, recorded at a distance of 43.6 km from ground zero, is shown in Figure 3.29. Note that the same pulse shape was recorded at this distance as at 18.6 km (Fig. 3.3).

Shot No. 4

Figure 3.6 shows a pulse recorded from an 11-kiloton weapon, detonated at a height of 6022 feet above the earth. Note that this waveform is not the same as those recorded from bombs detonated on top of a 300-foot tower. Although the first half cycle is in the negative direction, this component is of much shorter time duration than for Shots No. 2 and 3. The peak field strength of about 86 v/m seems to be low, considering the yield of the bomb. The frequency function, Figure 3.9, indicates an energy peak at a frequency near 28 kc. A record made with the gain controls set in expectation of a larger field strength is shown in Figure 3.30; Figure 3.31, which was recorded using a fast sweep rate, details the negative portion of the pulse. Figure 3.32 is a vertical incidence measurement, indicating that the original horizontally-polarized component was reflected from an ionospheric layer height of about 85 km. Figure 3.33 is a record of responses to the pulse by narrow-band receivers tuned to 2, 5 and 15 Mc. The timing marks are recorded on the bottom trace. Figure 3.34 is the same pulse recorded in the presence of noise at Site 7.1B, 43.6 km from the source. The arrow indicates the waveform which is thought to be the desired one, because it has the same shape as that shown in Figure 3.6. The positive peak value of field strength in Figure 3.34 is about 50 v/m; however, that of Figure 3.6 is about 86 v/m. The antennas used at the two sites were of the same length, but only the antenna at the main site was calibrated. The difference in field strengths may be due to the fact that the two antennas were at different heights above the earth.

Shot No. 5

Figure 3.7 is a pulse recorded from the second small bomb, which had a yield of about 0.22 kilotons, and was detonated from the top of a 100-foot tower. An automatic camera shutter closing mechanism produced the noise pulses which are seen as three horizontal lines extending across the photograph. The first half-cycle

[redacted]

is again in the negative direction and has a duration of about 7 μsec. The frequency function, Figure 3.10, corresponding to this waveform, has a peak in energy at a frequency near 35 kc. The same pulse, shown in Figure 3.8, was recorded at a distance of 46.5 km from the source. This waveform is similar to that in Figure 3.7, indicating that it did not change materially at twice the propagation distance. It would be expected that the higher frequency components might be more highly attenuated at the greater distance, but this trend is not evident from a comparison of the two frequency functions in Figures 3.10 and 3.11. Reflections from the hills immediately behind Site 7.1B may have slightly altered the waveform in Figure 3.8 after about 5 μsec. The rise time of the negative pulse is shown in Figures 3.36 and 3.37; the latter was recorded using a 0.3 μsec sweep delay time.

Shot No. 6

Figure 3.12 shows the pulse recorded at a range of 27.1 km from a 24-kiloton weapon, which was detonated from a 300-foot tower. The first half-cycle is in the negative direction and has a duration of about 18 μsec, and the frequency function, Figure 3.13, peaks at about 15 kc. The same pulse, recorded with a sweep speed of 5 μsec/cm, is seen in Figure 3.38; the total sweep time was not of sufficient length to permit the trace to return to the zero axis. Figure 3.39 shows the rise time of the negative phase of the pulse, using a sweep rate of 1 μsec/cm and a total sweep delay time of about 0.4 μsec. The peak field strength recorded at 50 km (Fig. 3.42) is 1.2 times greater than that recorded at a distance of 27 km (Fig. 3.12). This inconsistency in peak field strength was also observed for Shot No. 4. Since an antenna calibration was made at the 27-km site and not at the 50-km site, the values of field strength recorded at the 27-km site are more reliable. Figure 3.40, obtained using a sweep delay of .4 μsec and very high gain, reveals a small positive component immediately preceding the large negative phase. The cause of this positive movement is not known, but it was also recorded at another station operated by the Los Alamos Scientific Laboratory [4]. Figure 3.41 is a record showing responses to the pulse by narrow-band receiver tuned to 5 and 2 Mc. On the timing trace a seconds mark is shown on the extreme right, and a 40 msec timing mark appears immediately below the 2 Mc receiver response. Figure 3.42 is similar to Figure 3.39, except that the latter was recorded using an external delay line which gave a sweep delay of 0.2 μsec.

[redacted]

OSD
Section 6.2 (a)

DOE
Section 6.2(a)

Shot No. 7

This weapon, having a yield of about 43 kilotons, was detonated atop a 300-foot tower. [redacted] The record in Figure 3.45 was obtained with an overall sweep delay time of 0.4 μsec; a very high gain was used so that the main negative phase saturated the equipment. The early detail consisted of an initial negative pulse, followed by a small positive pulse, and finally by the main negative one. This detail was also observed by the Los Alamos Scientific Laboratory group at a separate site. Figure 3.46 shows the response to the pulse recorded from the narrow-band receivers, tuned to frequencies of 3 and 2 Mc and also shows the time reception of these pulses as determined from the timing marks on the bottom trace.

Shot No. 8

Shot No. 8 was a 26-kiloton weapon detonated at a height of 2423 feet above the earth. [redacted] A Tektronix 517 oscilloscope, on loan from the Los Alamos Scientific Laboratory for only Shot No. 8, was used to record the rise time of this pulse. Since the 517 oscilloscope is capable of reproducing pulses with faster rise times than the 513-D oscilloscope, an attempt was made to compare the rise times recorded by the two sets of equipment. Unfortunately, this comparison was not successful because ringing occurred in an antenna lead common to all 513-D oscilloscopes, see Figures 3.47 and 3.48, and too much gain was used in the 517 oscilloscope, which was driven near the point of saturation at the 37 v/m level. The peak amplitude of this pulse was about 300 v/m (Fig. 3.14).

Shot No. 9

The pulse recorded at a distance of 14 km from this 27-kiloton weapon, which was detonated from a 300-foot tower, is shown in Figure 3.18. The peak of the frequency function of this pulse (Fig. 3.21) occurs at about 17 kc. The pulse, recorded at the same distance but

[redacted]

[redacted]

at a different site, is seen in Figure 3.52. The waveforms of both are very similar, and the peak value of field strength is about 648 v/m in both cases. High-frequency responses recorded at frequencies of 5 and 2 Mc, and the timing trace, are shown in Figure 3.51.

Shot No. 10

Figure 3.19 shows the pulse recorded at 18.5 km from the 15-kiloton cannon shot, which was detonated at a height of about 300 feet above the earth. The negative half cycle is seen to have a sharp spike which was not usual with the 300-foot tower shots. This same spike is also evident in Figure 3.53, which was recorded at a distance of 14.4 km. The waveforms of both pulses are similar; each has a negative peak amplitude of about 580 v/m. The peak of the frequency function, Figure 3.22, for the pulse shown in Figure 3.19, occurs at about 24 kc. Figure 3.54 shows the rise time of the negative phase, using a sweep delay time of 0.4 μsec. The same pulse, recorded at a different site, is shown in Figure 3.56. The peak amplitudes of both negative pulses are about 590 v/m. Figure 3.55 is the narrow-band record, showing high-frequency responses at 5 and 2 Mc. Figure 3.57 is a record of early rise rate, using high gain and a 0.4 μsec sweep delay time. No positive or negative precursors were recorded in advance of the main negative pulse. This result was confirmed by members of the Los Alamos Scientific Laboratory.

Shot No. 11

Shot No. 11, having a yield of about 61 kilotons, was an air drop detonated at a height of 1350 feet above the earth. The recorded pulse is shown in Figure 3.20, and its frequency function is shown in Figure 3.23, with a peak at about 18 kc. A comparison of this record with that of Shot No. 4, another air drop (Fig. 3.6), reveals some significant differences. The radiation pattern from a high air drop might be different from that of a low air drop, and due to different angles of reflection from the ground, differences in the waveforms of received pulses would be produced . The record shown in Figure 3.58 reveals the rise time of the negative phase of the pulse. This record was made using a 0.4 μsec sweep delay time. Figure 3.59 shows the positive detail recorded in advance of the main negative phase. This record was made using a 0.4 μsec sweep delay time, and it was necessary to use a very high gain in order to see these small positive precursors.

[redacted]

[redacted]

OSD
Section 6.2 (a)

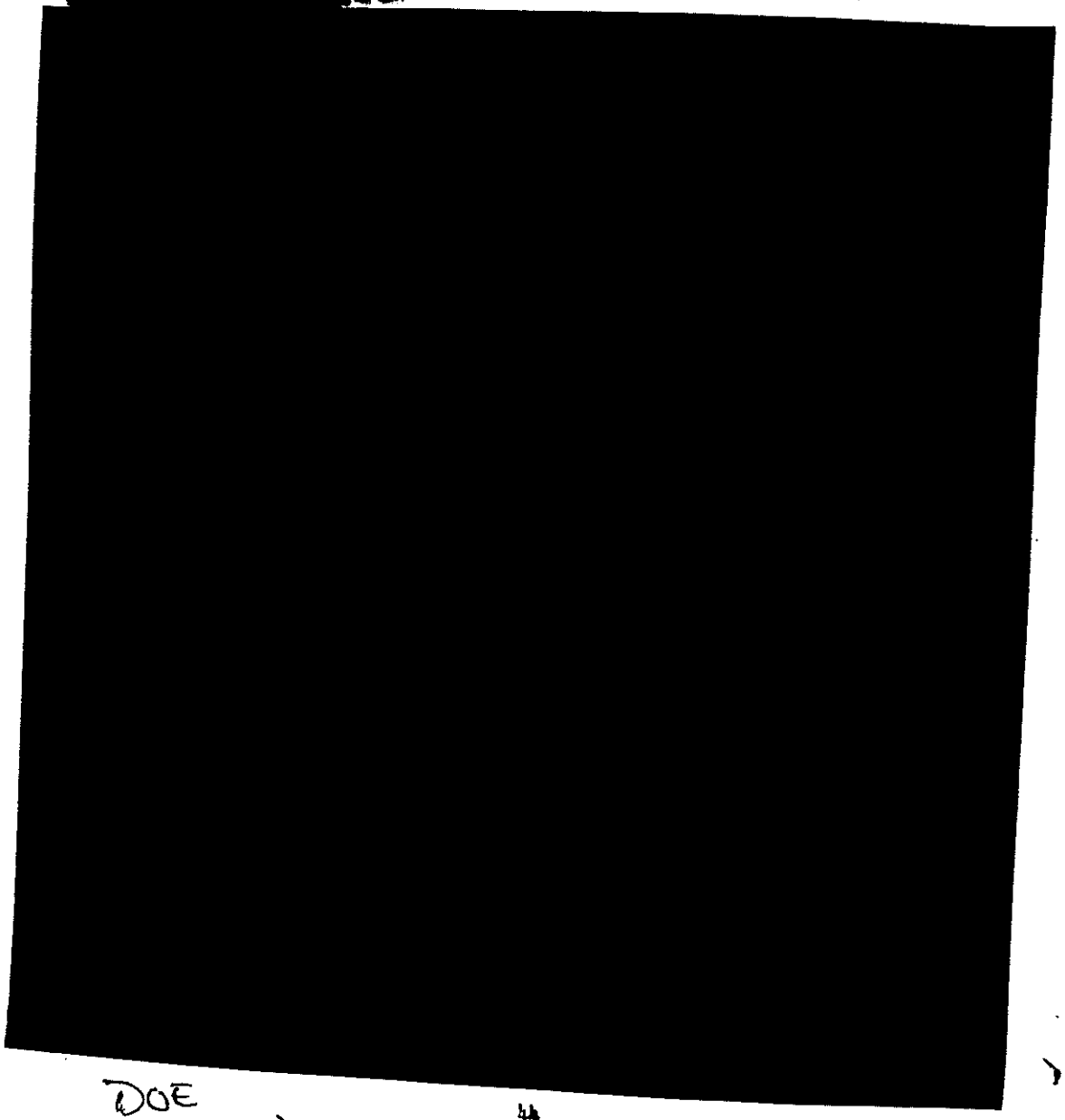

DOE
Section 6.2(a)

[redacted]

[redacted]

FREQUENCY FUNCTIONS OF BROADBAND PULSES ON PREVIOUS PAGE

No frequency function available
Shot No. 1

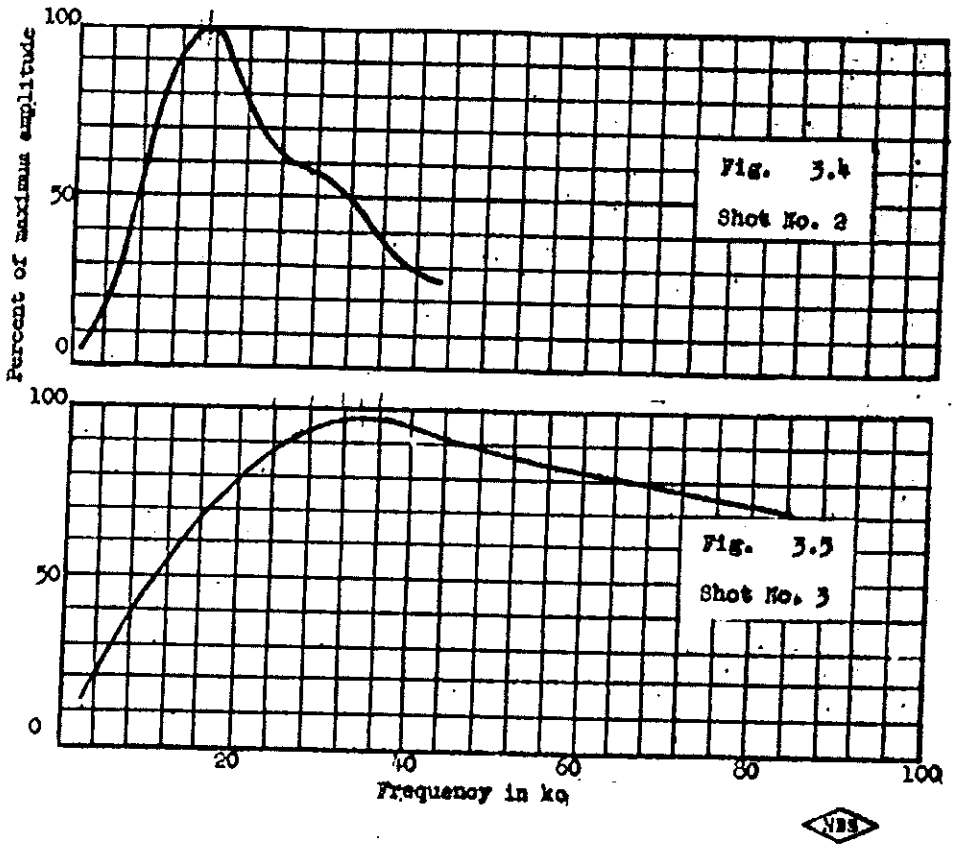

[redacted]

OSD
Section 6.2 (a)

[redacted]

DOE
Section 6.2(a)

[redacted]

FREQUENCY FUNCTIONS OF BROADBAND PULSES ON PREVIOUS PAGE

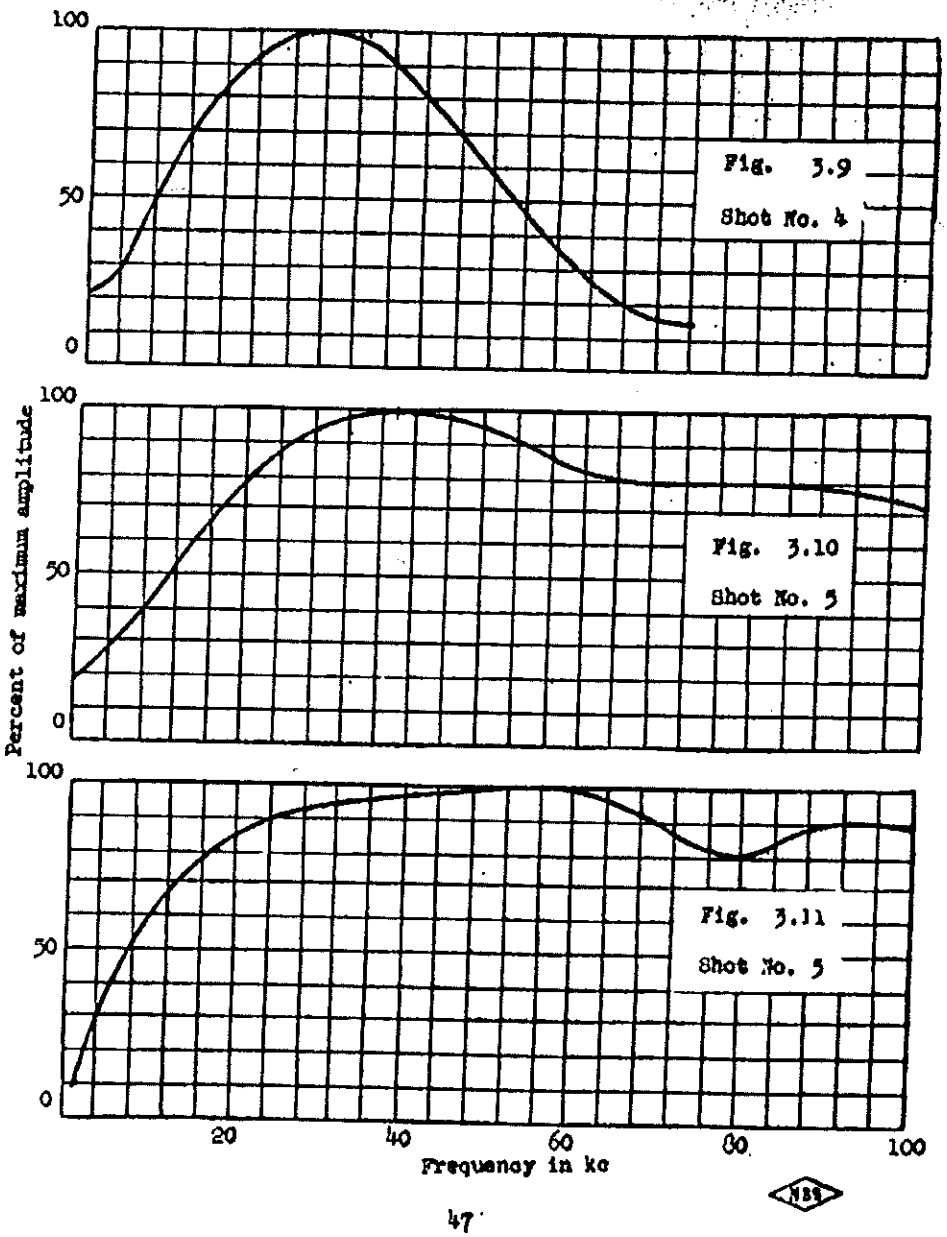

OSD
Section 6.2 (a)

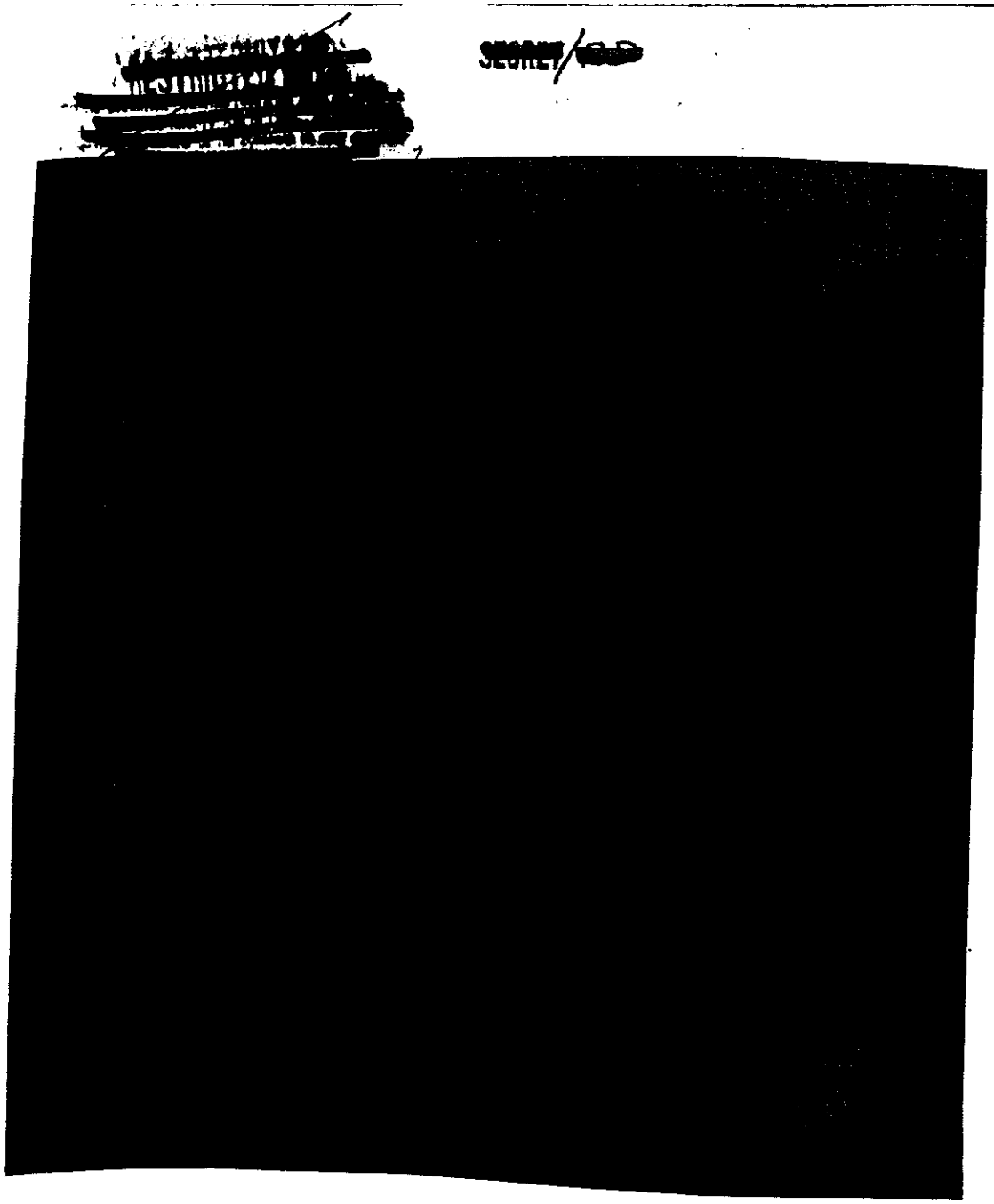

DOE
Section 6.2(a)

[redacted]

FREQUENCY FUNCTIONS OF BROADBAND PULSES OF [redacted]

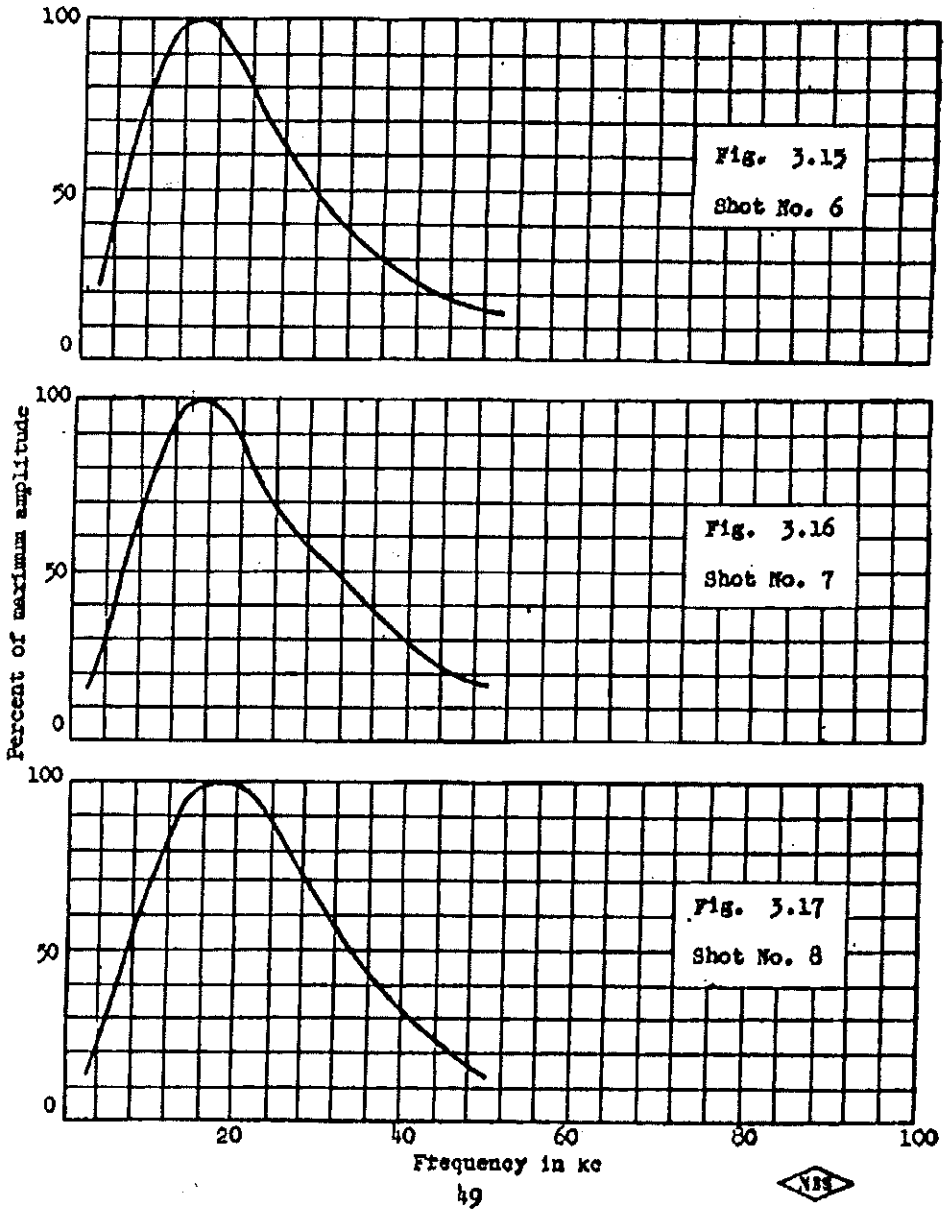

[redacted]

OSD
Section 6.2 (a)

[redacted]

[redacted]

DOE
Section 6.2(a)

[redacted]

[redacted]

FREQUENCY FUNCTIONS OF BROADBAND PULSES ON PREVIOUS PAGE

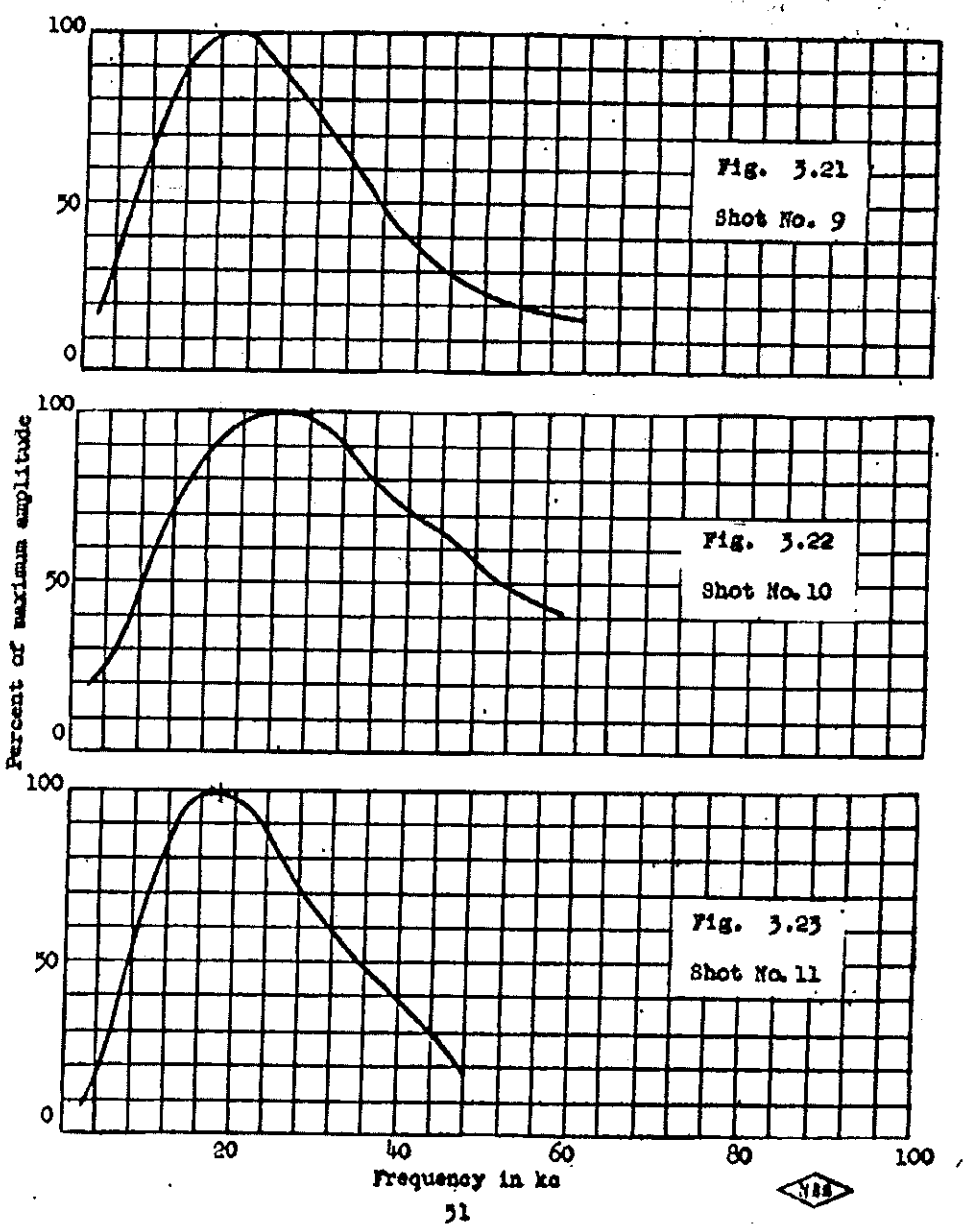

[redacted]

OSD
Section 6.2 (a)

[redacted]

SECRET/[redacted]

[redacted]

DOE
Section 6.2(a)

SECRET/[redacted]

OSD
Section 6.2 (a)

[redacted]

[redacted]

DOE
Section 6.2(a)

[redacted]

OSD
Section 6.2 (a)

[redacted]

[redacted]

DOE
Section 6.2(a)

[redacted]

OSD
Section 6.2 (a)

[redacted]

DOE
Section 6.2(a)

[redacted]

[redacted]

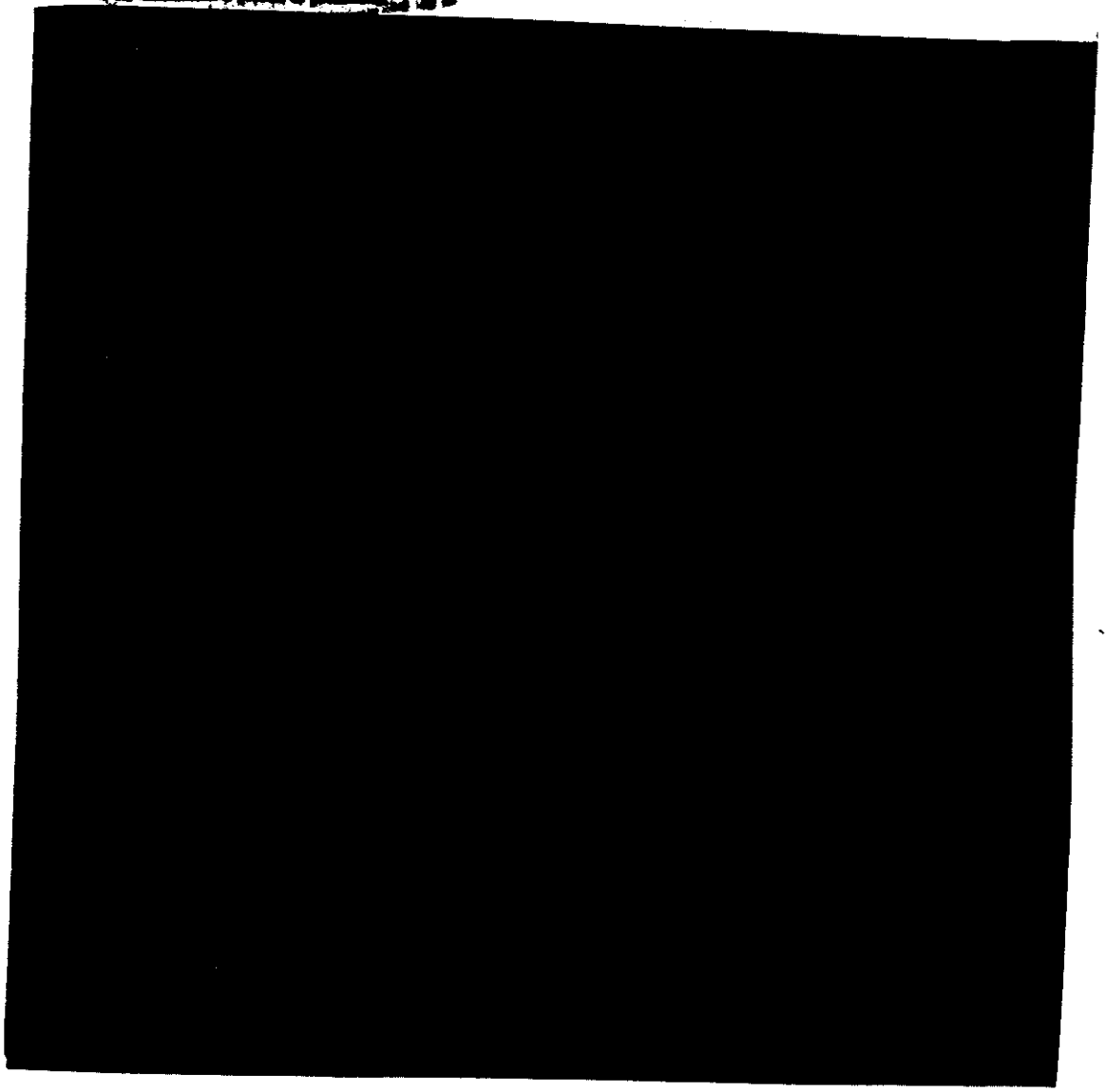

DOE
Section 6.2(a)

[redacted]

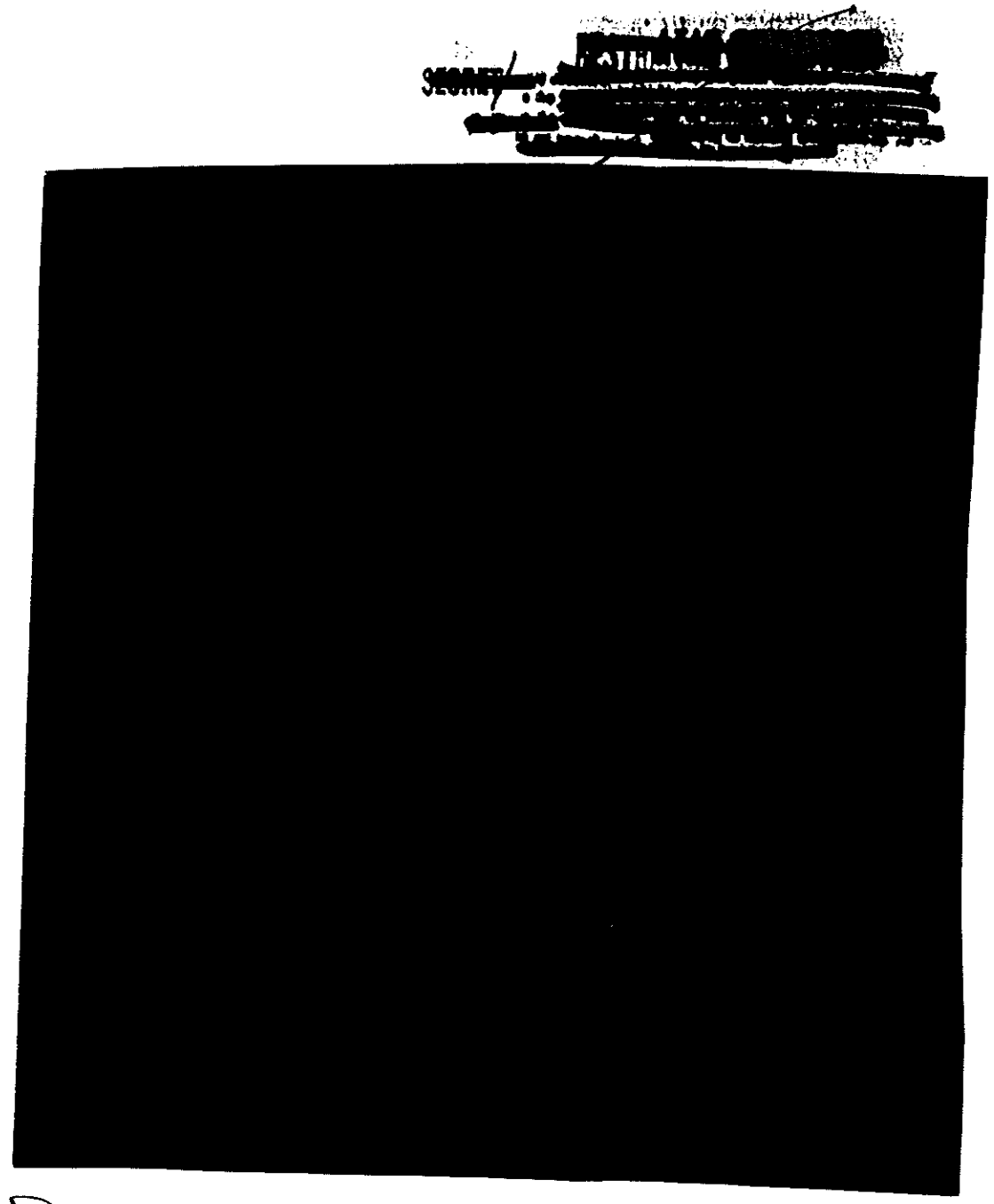

DOE
Section 6.2(a)

OSD
Section 6.2 (a)

[redacted]

[redacted]

DOE
Section 6.2(a)

[redacted]

OSD
Section 6.2 (a)

[redacted]

DOE
Section 6.2 (a)

[redacted]

[redacted]

[redacted]

OSD
Section 6.2 (a)

[redacted]

DOE
Section 6.2(a)

60

[redacted]

[redacted]

OSD
Section 6.2 (a)

[redacted]

DOE
Section 6.2(a)

[redacted]

[redacted]

SECRET/[redacted]

OSD
Section 6.2 (a)

[redacted]

DOE
Section 6.2(a)

62

SECRET/[redacted]

OSD
Section 6.2 (a)

SECRET/[redacted]

[redacted]

DOE
Section 6.2(a)

(S)

SECRET/[redacted]

[redacted] SECRET

3.7.2 Discussion of Boulder Records

All of the narrow-band records recorded at Boulder are similar in appearance. The very-low-frequency receivers were tuned to 15 and 30 kc throughout the test series, whereas the high-frequency receiver was tuned to a channel near the maximum usable frequency. Figure 3.73 is a typical record of narrow-band receiver responses. The responses recorded at 15 and 30 kc have a steep front and a slow decay time, due to ringing produced in the receivers. The receiver output response is independent of the shape of the received pulse; however, the peak amplitude of the receiver response is related to the energy of the received pulse. Oscilloscope grid lines were photographed with the pulses and appear in the illustrations as equally spaced horizontal lines. The response recorded at a frequency of 2.99 Mc is composed of a number of individual pulses which arrived at different intervals of time, depending upon the number of modes reflected from the ionosphere, and the propagation delay for each. The film speed of 17 in/sec is too slow to clearly separate these individual pulses since the time intervals are of the order of 100 μsec. A 40 msec time interval is shown, and it is terminated by a one second mark. The smaller square pulse on the time trace is the pulse gate output mark from the Tektronix oscilloscope and indicates that the broadband receiver recorded a pulse at that time.

Figure 3.73 shows a time comparison made between a WWV seconds mark (consisting of 5 cycles of 1000 cps) and a seconds pulse from the timing unit. Note that the pulse from the timer lags the beginning of the WWV seconds pulse by about 1.6 milliseconds. This lag was corrected by adjusting a phase shifting control on the frequency divider unit. A better agreement is shown in Figure 3.77. In Figure 3.70 a seconds pulse from station WWV is followed by a seconds pulse received from WWVH about 10.6 milliseconds later. The timer unit was not in operation for Shot No. 8 at Boulder. It was necessary to record station WWV directly on the timing trace as seen in Figure 3.83. Note that the 440 cps steady tone ends just before the pulses from the detonation were recorded. The large pulse on the timing trace was also received from the detonation at a frequency of 5 Mc.

Details of the shape of the pulse for Shot No. 6, as recorded by the broadband equipment, are shown in Figure 3.74. Note that the first half cycle is negative. The duration of the main part of the waveform is about 262 μsec, but a half cycle of small amplitude is seen to occur at about 450 μsec. The second half

[redacted]

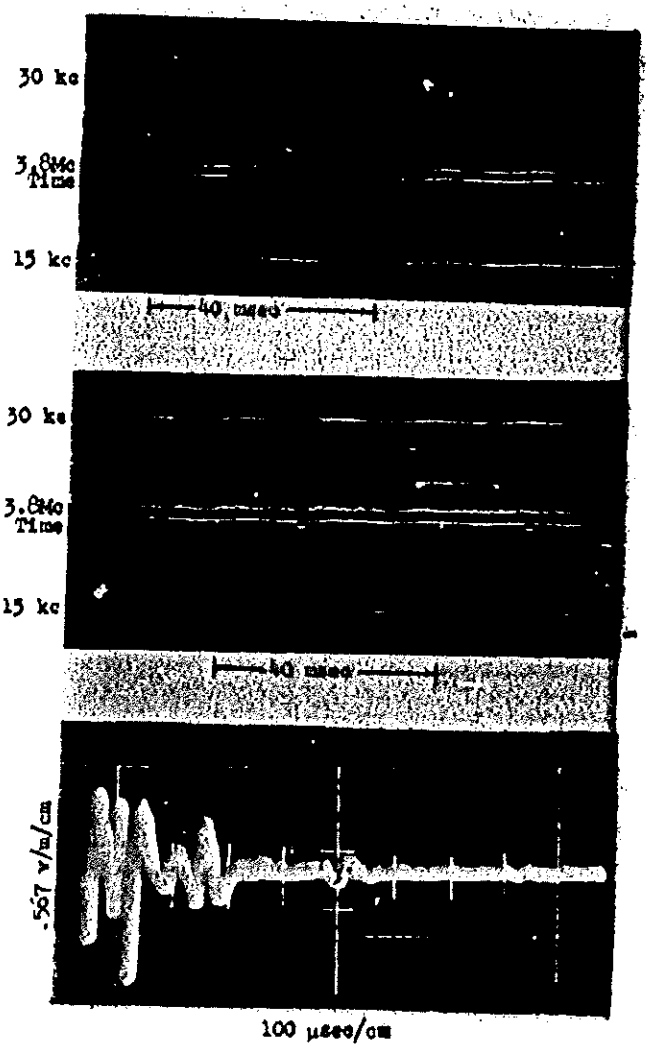

Fig. 3.60

Narrow-band responses

Shot No. 1

1000 km from ground zero

Fig. 3.61

Narrow-band responses

Shot No. 2

1000 km from ground zero

Fig. 3.62

Broadband pulse

Shot No. 2

1000 km from ground zero

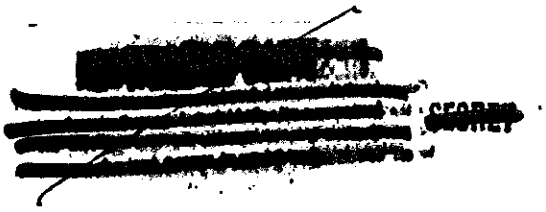

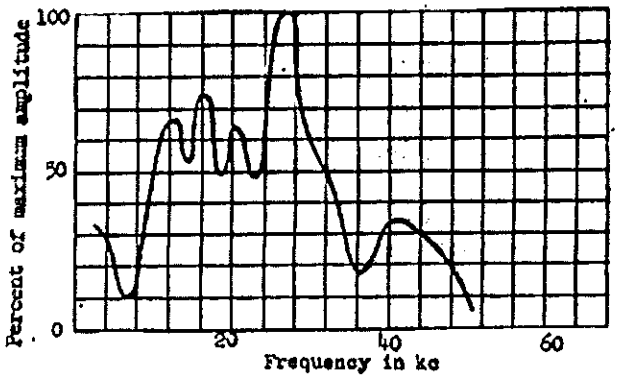

Fig. 3.63

Frequency function of broadband pulse

Shot No. 2

1000 km from ground zero

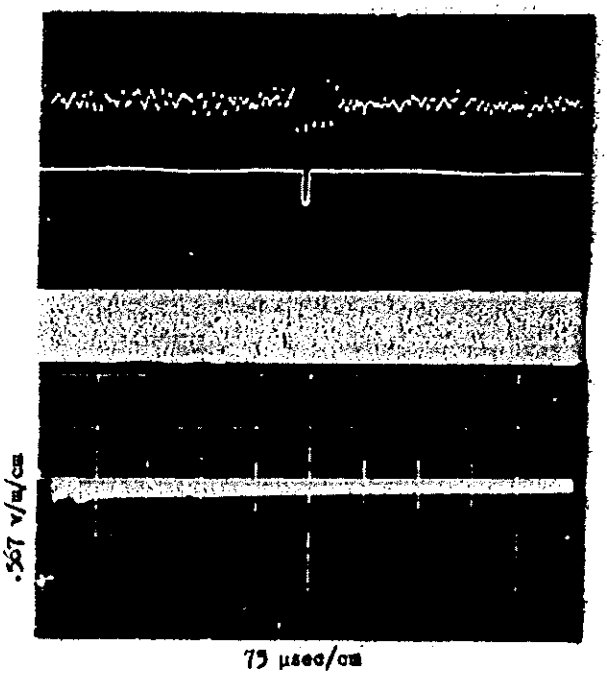

Fig. 3.64

Time comparison of second marks from WWV (top) and timer unit

Shot No. 2

1000 km from ground zero

Fig. 3.65

Broadband pulse

Shot No. 3

1000 km from ground zero

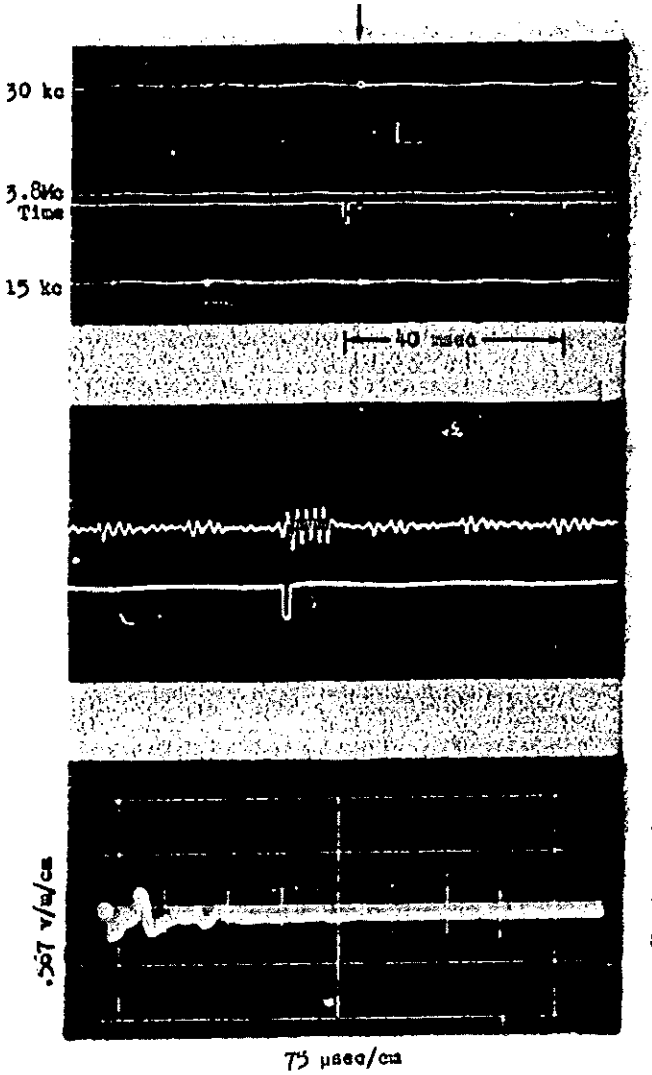

Fig. 3.66

Narrow-band responses

Shot No. 3

1000 km from ground zero

Fig. 3.67

Time comparison of second marks from WWV (top) and timer unit

Shot No. 3

1000 km from ground zero

Fig. 3.68

Broadband pulse

Shot No. 4

1000 km from ground zero

NBS

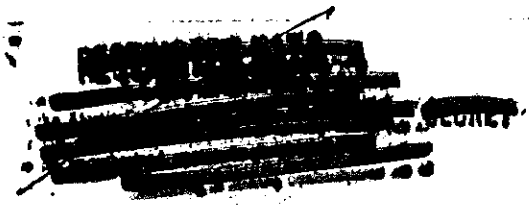

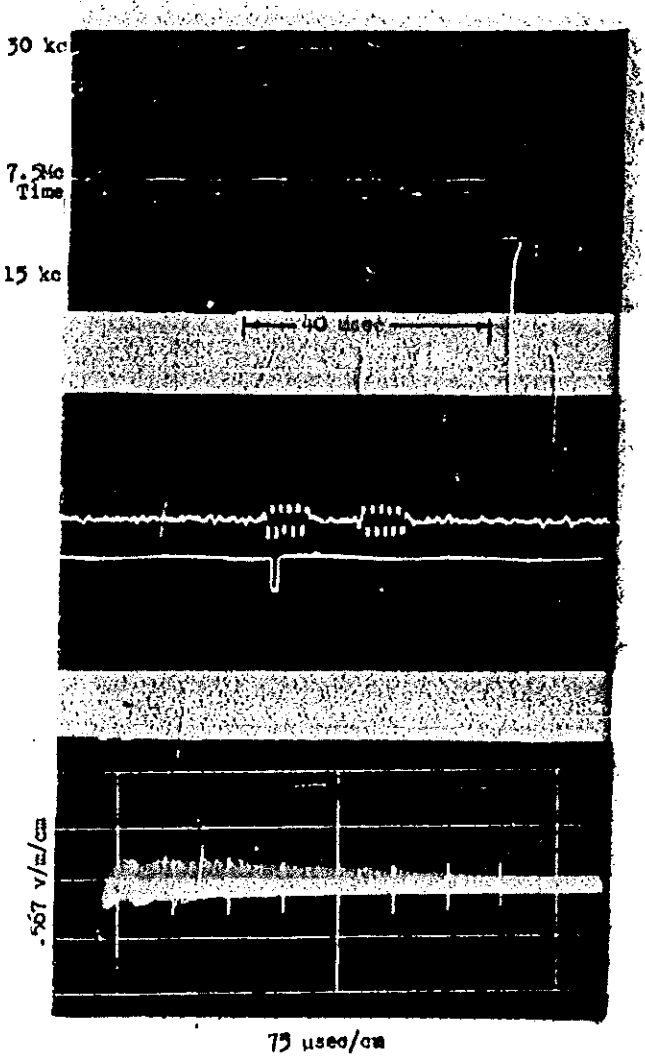

Fig. 3.69

Narrow-band responses

Shot No. 4

1000 km from ground zero

Fig. 3.70

Time comparison of second marks from WWV (top) and timer unit

Shot No. 4

1000 km from ground zero

Fig. 3.71

Broadband pulse

Shot No. 5

1000 km from ground zero

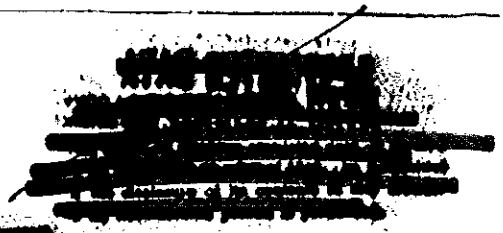

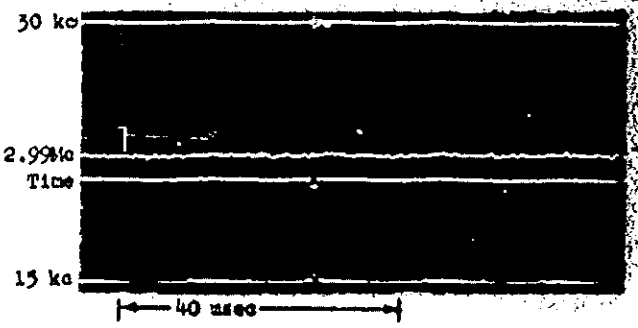

Fig. 3.72

Narrow-band responses

Shot No. 5

1000 km from ground zero

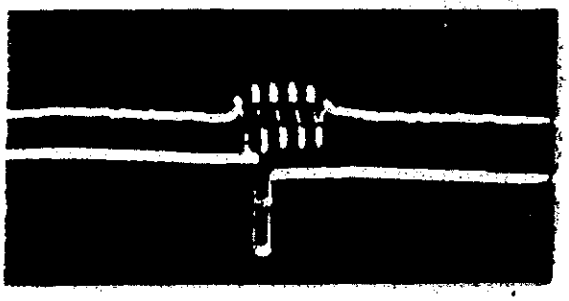

Fig. 3.73

Time comparison of second marks from WWV (top) and timer unit

Shot No. 5

1000 km from ground zero

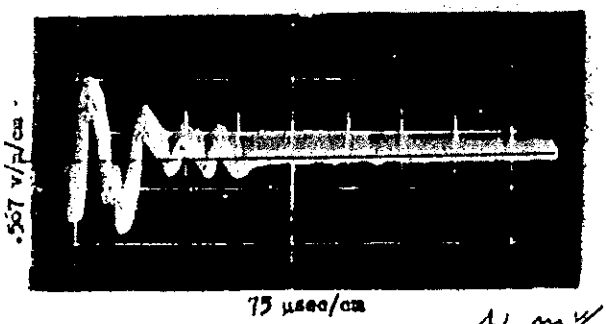

Fig. 3.74

Broadband pulse

Shot No. 6

1000 km from ground zero

41 mv/m at 13 kc (ZOMBI)

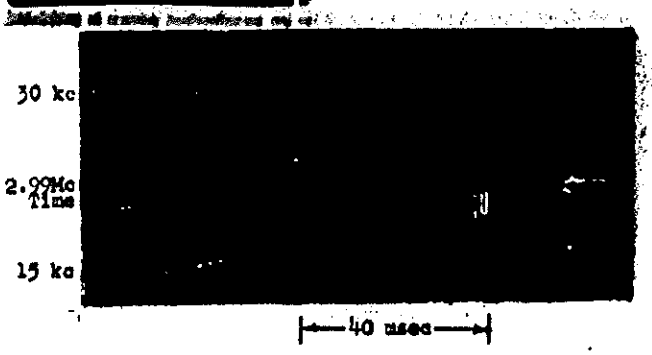

Fig. 3.75

Narrow-band responses

Shot No. 6

1000 km from ground zero

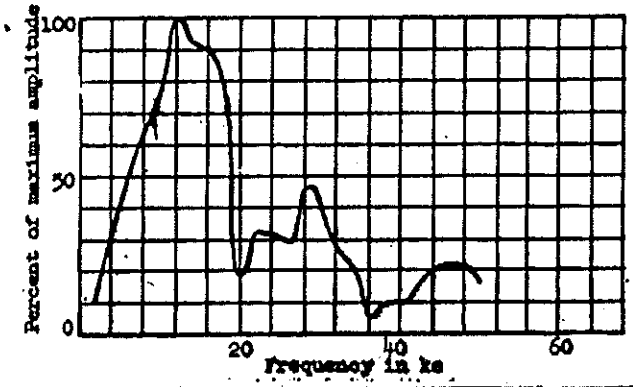

Fig. 3.76

Frequency function of broadband pulse

Shot No. 6

1000 km from ground zero

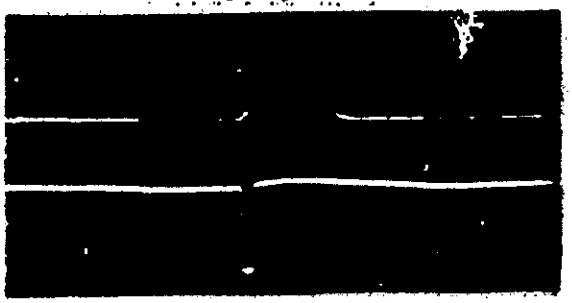

Fig. 3.77

Time comparison of second marks from WWV (top) and timer unit

Shot No. 6

1000 km from ground zero

[redacted]

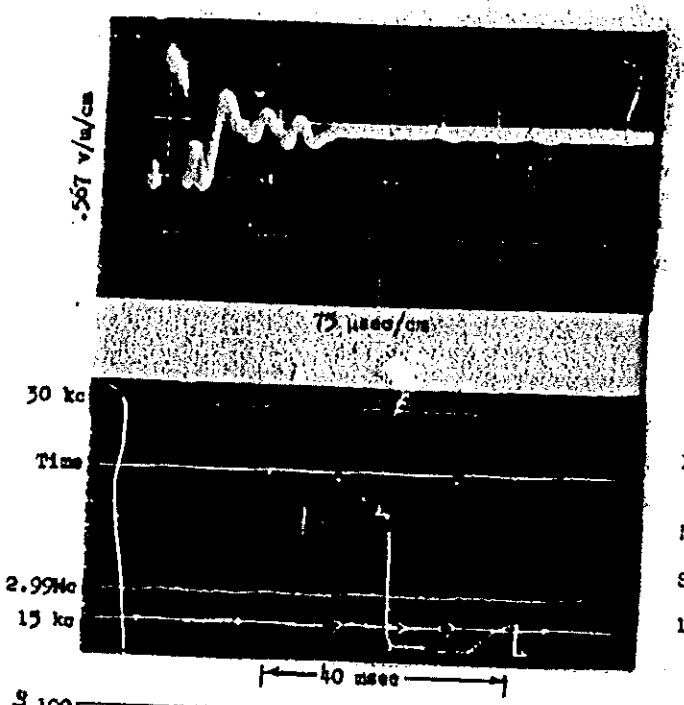

42 mv/m
AT 13 kc
(Boost)

Fig. 3.78
Broadband pulse
Shot No. 7
1000 km from ground zero

Fig. 3.79
Narrow-band responses
Shot No. 7
1000 km from ground zero

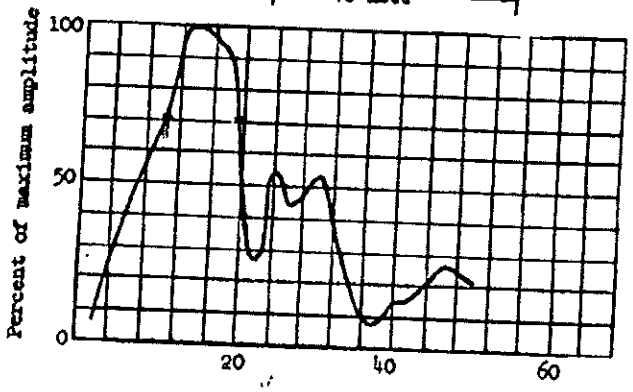

Fig. 3.80
Frequency function of broadband pulse
Shot No. 7
1000 km from ground zero

NRL

[redacted]

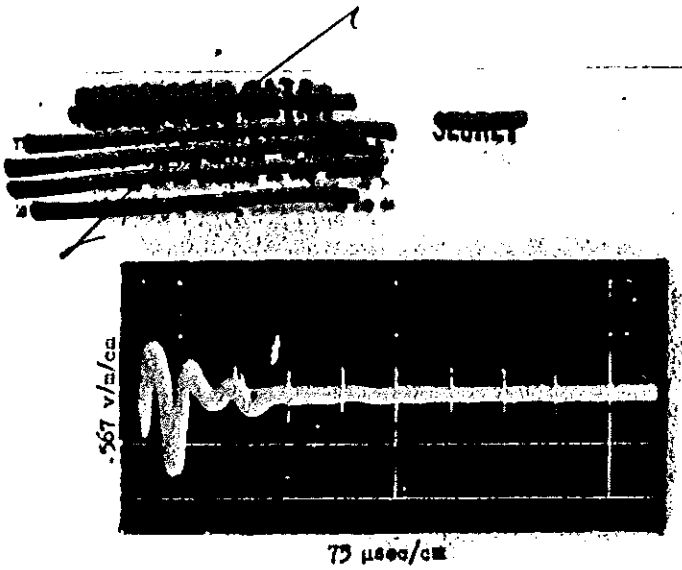

Fig. 3.81

Broadband pulse

Shot No. 8

1000 km from ground zero

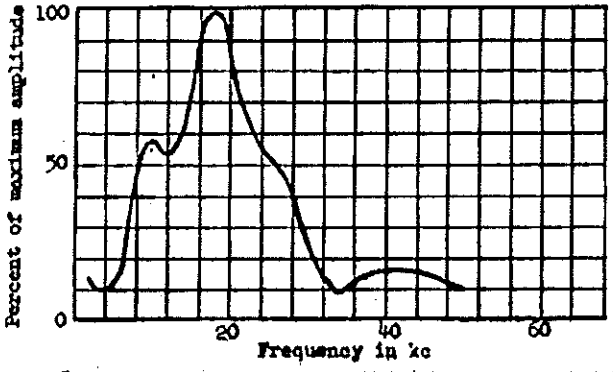

Fig. 3.82

Frequency function of broadband pulse

Shot No. 8

1000 km from ground zero

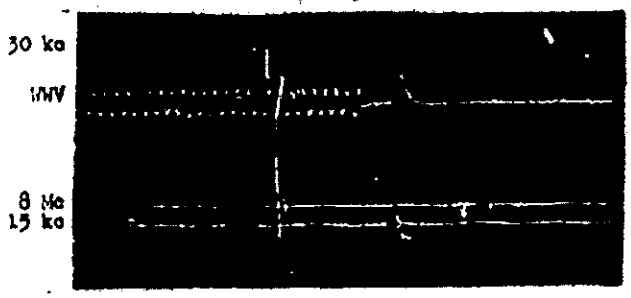

Fig. 3.83

Narrow-band responses

Shot No. 8

1000 km from ground zero

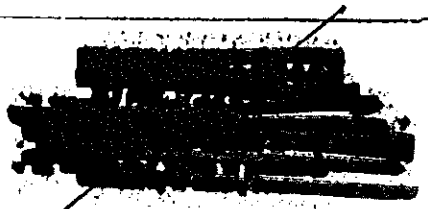

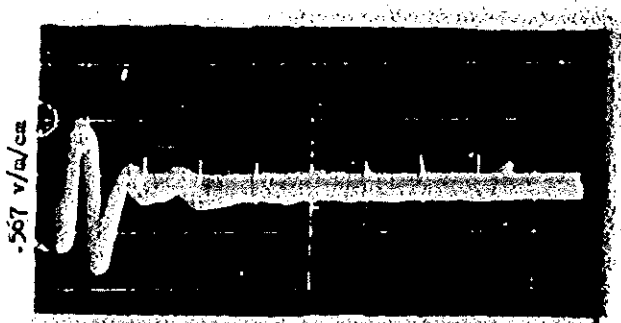

Fig. 3.84

Broadband pulse

Shot No. 9

1000 km from ground zero

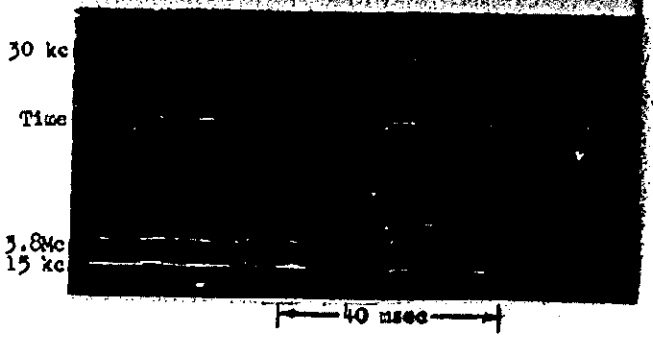

Fig. 3.85

Narrow-band responses

Shot No. 9

1000 km from ground zero

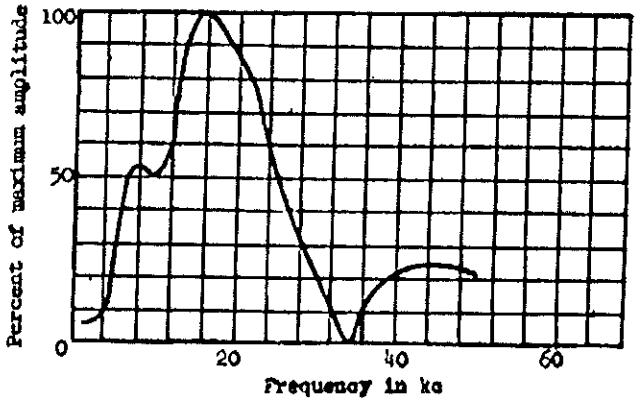

Fig. 3.86

Frequency function of broadband pulse

Shot No. 9

1000 km from ground zero

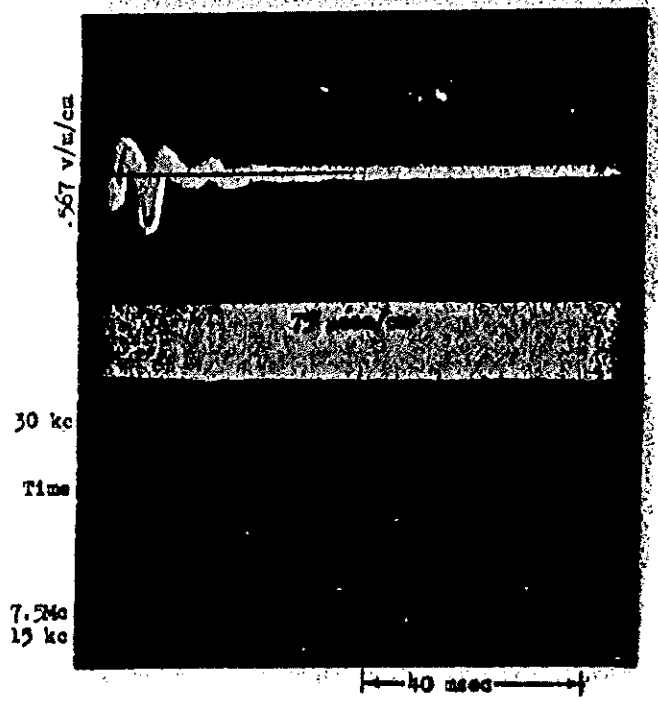

Fig. 3.87

Broadband pulse

Shot No. 10

1000 km from ground zero

Fig. 3.88

Narrow-band responses

Shot No. 10

1000 km from ground zero

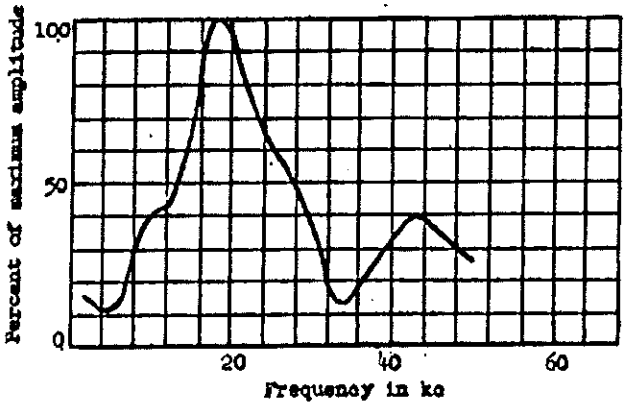

Fig. 3.89

Frequency function of broadband pulse

Shot No. 10

1000 km from ground zero

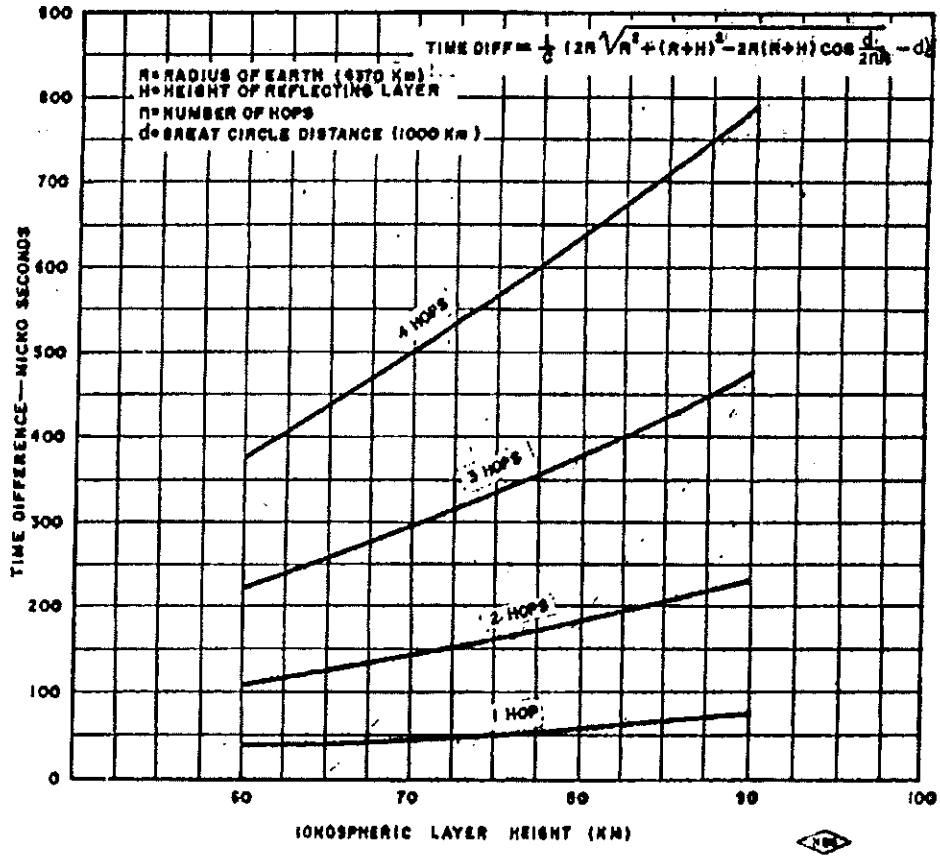

FIG. 3.90 TIME INTERVAL BETWEEN PROPAGATION MODES VS IONOSPHERIC LAYER HEIGHT FOR A 1,000 KM PATH

[redacted] SECRET

[redacted] has a peak amplitude of about 0.67 v/m. In Figure 3.76, which is the frequency function for this pulse, it is seen that the peak of the frequency function is near 12 kc. Comparison of the waveform of this pulse with that recorded at a distance of 27 km, at the Nevada Proving Ground (Fig. 3.12), shows that the one recorded at 1000 km is about 4 times as long, and appears to be composed of a series of pulses of the type recorded at 27 km. By comparing the frequency functions of these pulses recorded at the Nevada Proving Ground with those recorded at Boulder, Colorado, the effects of propagation can be seen. The peak frequency is shifted by propagation from about 15 kc to about 12 kc, and the frequency components above 16 kc are strongly attenuated. By comparison, the amplitude of the frequency components below 12 kc are not attenuated nearly as much as those above 16 kc. Thus, the effect on the waveform produced by propagation is similar to that produced by a low pass filter.

Additional records obtained at Boulder, which may be interpreted in the same manner, appear in Figures 3.78, 3.81 and 3.84. Figure 3.90 is a chart plotted to give propagation delay times between successive modes over a 1000 km path as a function of ionospheric layer height, parametric in number of ionospheric reflections. This chart was used to explain the composition of the pulse shown in Figure 3.74. From this chart, assuming a layer height of 80 km, the first-hop sky wave will arrive about 60 μsec later than the ground-wave component. Similarly, the second-hop sky wave will be delayed 185 μsec, the third hop 380 μsec and the fourth hop 640 μsec, with respect to the ground wave arrival time. It is reasonable to attribute the first two half-cycles of the pulse in Figure 3.74 to ground wave and the latter portion to sky wave. A change in waveform, consisting of 4 half cycles, occurs after about 60 μsec, corresponding to the time of arrival of the first-hop sky wave. The first-hop sky wave arrived with an apparent reversal in phase. Some workers[2] claim that the first-hop sky wave is received with a phase reversal. Likewise a change occurs after 185 μsec, corresponding to the arrival time of the second-hop sky wave. The two half cycles of small amplitude, beginning after 640 μsec, correspond to the time of the arrival of the third-hop sky wave. The calculated time of arrival for the third-hop sky wave is 300 μsec and approximates the beginning time of a series of about 6 half cycles of very small amplitude. No further oscillations, due to higher propagation modes, are discernable.

[redacted]

The time intervals used in the above analysis correspond to a layer height of 70 km which is a reasonable value for very low frequencies. It is known[6] that an effect produced by sunrise along the propagation path is a decrease in the reflection height. Since sunrise occurred along the path of propagation for the pulse under consideration, it is likely that different reflection heights would be obtained for each mode. For this reason, the use of propagation delay intervals corresponding to a constant layer height is not rigorously correct. The low number of sky-wave reflections is evidence of high absorption along the path. Under conditions of low absorption along an all-darkness path, it is not unusual to receive ten or more modes of reflection from distant atmospherics.

3.1.3 Discussion of Washington, D. C. Records

Figure 3.98 is typical of the narrow-band receiver responses recorded at Ft. Belvoir. Two U. S. Navy type RBA tuned-radio-frequency receivers, each having a bandwidth of about 420 cps, were used to record pulses from detonations at frequencies of 16 and 30 kc. The lowest frequency receiver at Ft. Belvoir was tuned to 16 kc instead of 15 kc. However, by referring to the frequency functions of the pulses recorded at Boulder and Ft. Belvoir for Shots No. 9, 10 and 11, it can be seen that the difference in amplitudes received at frequencies of 15 and 16 kc is very small and may be neglected for the purposes of this report. The top trace shown in Figure 3.98 shows the response of the 30-kc receiver, which overlaps that of the 16 kc receiver. A very small signal was recorded at 10 Mc. A 40 msec time interval can be seen on the timing trace, and the pulse on the right is a seconds marker. The pulse on the timing trace at the detonation time is from the Tektronix oscilloscope, indicating that the broadband receiver recorded a pulse at that time. A few responses with small amplitude, due to distant atmospherics, can be seen on the 16 kc channel.

The pulses recorded by the broadband receivers at Ft. Belvoir can be interpreted in the same manner as those recorded at Boulder. It must be borne in mind that a band-rejection filter, centered on 18 kc, distorted all records from Shots prior to Shot No. 9. For example, see Figures 3.97, 3.99 and 3.101. For this reason frequency functions of the pulses are displayed only for Shots No. 9, 10 and 11. Suitable records, which were recorded at Boulder and Ft. Belvoir for Shots No. 9 and 10, show effects of ionospheric filtering. The pulses recorded at Ft. Belvoir are simpler in character than those recorded at Boulder. The minor

ripples on the traces, Figures No. 3.101, 3.103, 3.106, are due to interference and are not a part of the desired signal.

The ground wave attenuation (referred to the value at 1.6 km) for a 3400 km path is about 60 db over good earth. Therefore, the ground-wave pulse was not received at Ft. Belvoir. Using ray theory, the angle of arrival for the first-hop sky wave is a negative one, and there is no evidence that the first-hop sky wave was received at Ft. Belvoir. Assuming an ionospheric layer height of 80 km, there will be approximately a 50 μsec delay (see Fig. 3.112) between the arrival of the third- and fourth-hop sky wave and about 120 μsec delay between the fourth- and fifth-hop sky wave. Referring to Figure 3.106 it is assumed that the first two half-cycles correspond to the second-hop sky wave. The third half-cycle is seen to arrive about 50 μsec after the beginning of the first half-cycle, and the third and fourth half-cycles are taken to be the third-hop sky-wave reflections. Similarly, the fifth and sixth half-cycles correspond to the arrival time of the fourth-hop sky wave.

Reproductions of additional records obtained at Ft. Belvoir appear in Figures 3.91 to 3.111.

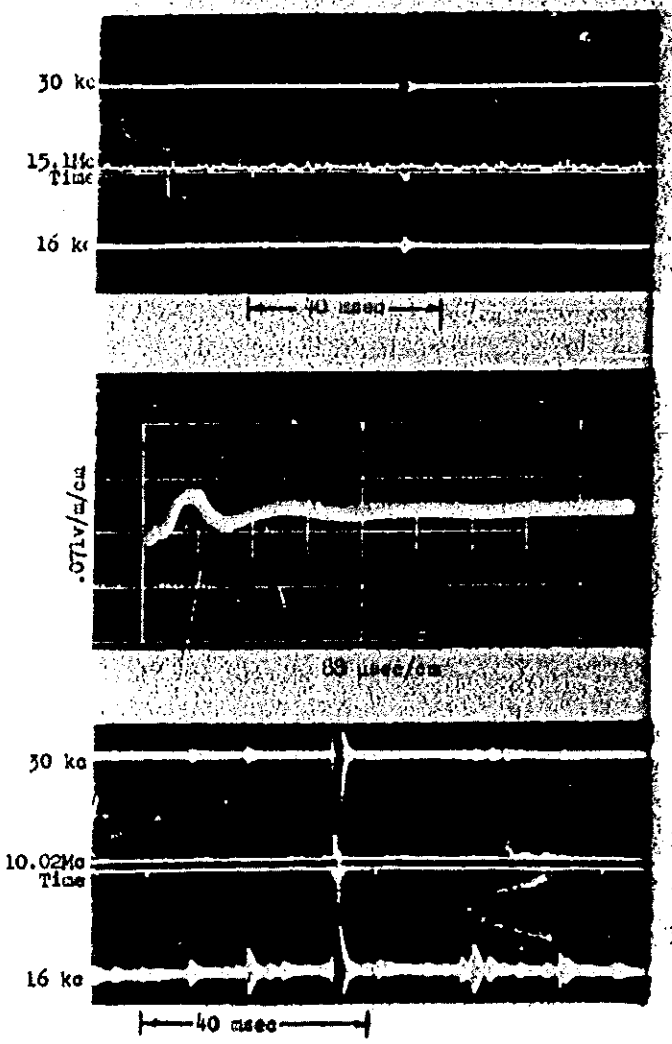

Fig. 3.91
Narrow-band responses
Shot No. 1
3400 km from ground zero

Fig. 3.92
Broadband pulse
Shot No. 2
3400 km from ground zero

Fig. 3.93
Narrow-band responses
Shot No. 2
3400 km from ground zero

[redacted]

[redacted]

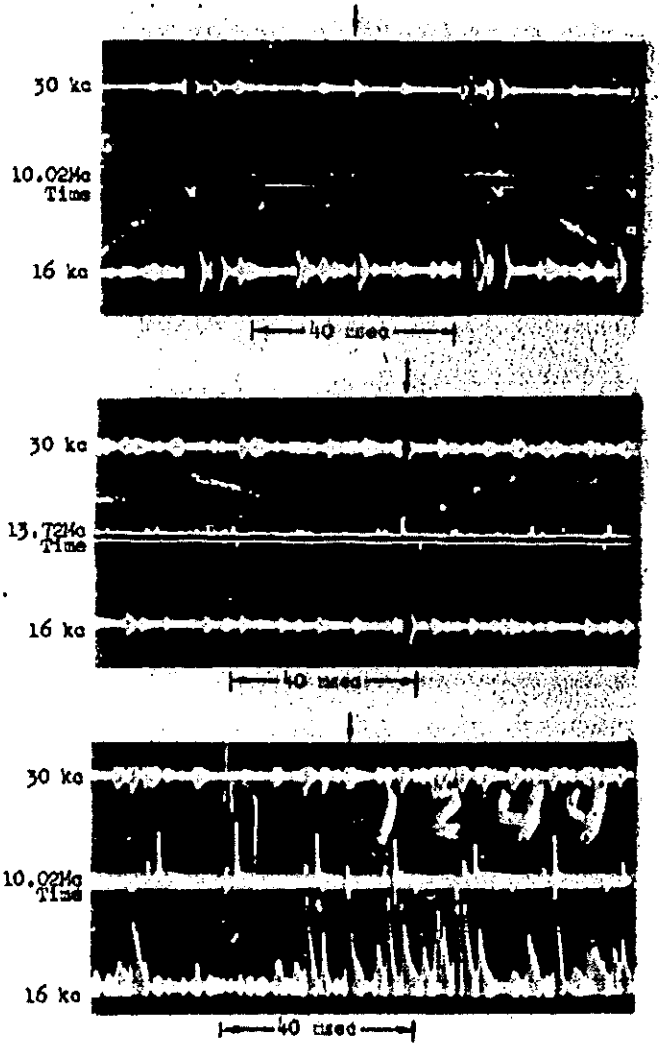

Fig. 3.94
Narrow-band responses
Shot No. 3
3400 km from ground zero

Fig. 3.95
Narrow-band responses
Shot No. 4
3400 km from ground zero

Fig. 3.96
Narrow-band responses
Shot No. 5
3400 km from ground zero

[redacted]

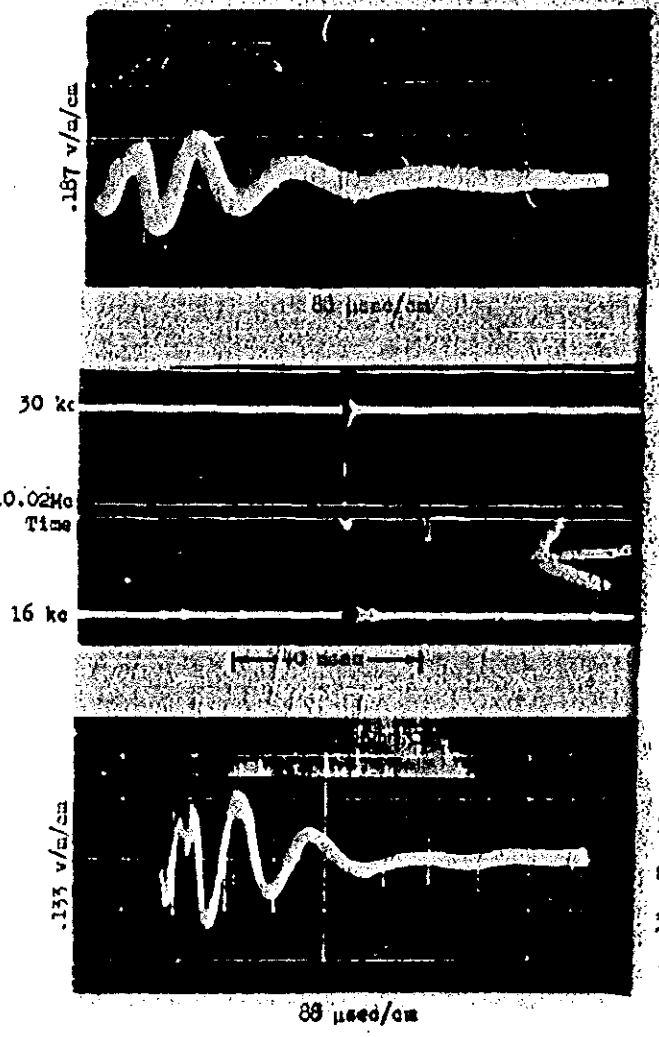

Fig. 3.97
Broadband pulse
Shot No. 6
3400 km from ground zero

Fig. 3.98
Narrow-band responses
Shot No. 6
3400 km from ground zero

Fig. 3.99
Broadband pulse
Shot No. 7
3400 km from ground zero

[redacted]

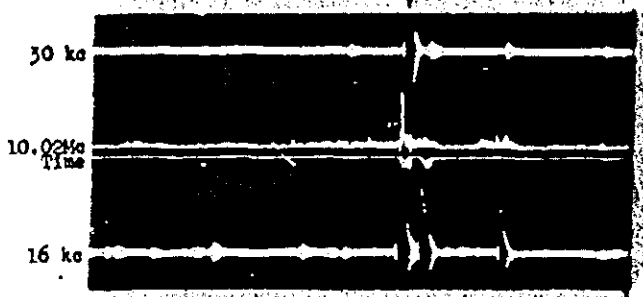

Fig. 3.100

Narrow-band responses

Shot No. 7

3400 km from ground zero

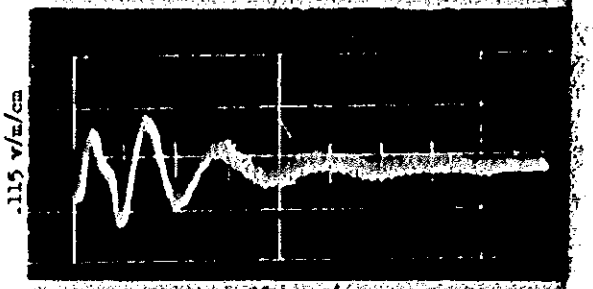

Fig. 3.101

Broadband pulse

Shot No. 8

3400 km from ground zero

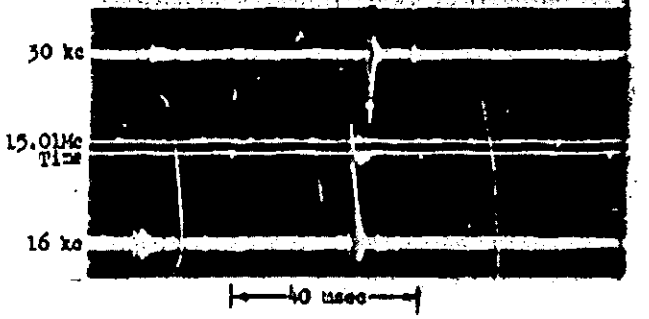

Fig. 3.102

Narrow-band responses

Shot No. 8

3400 km from ground zero

SECRET

[redacted]

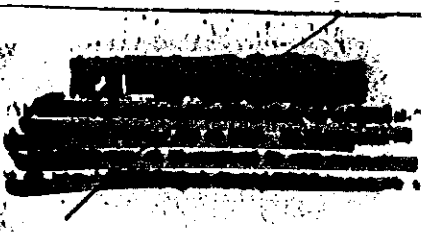

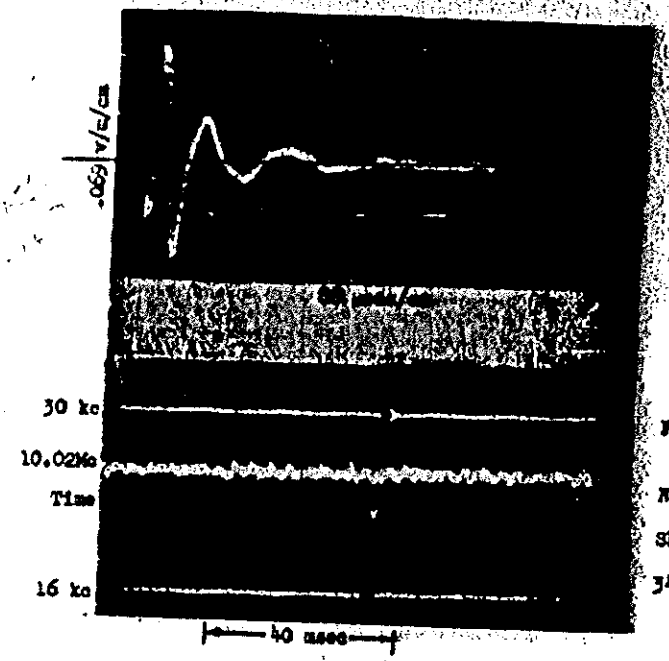

Fig. 3.10a

Broadband pulse

Shot No. 9

3400 km from ground zero

Fig. 3.10b

Narrow-band responses

Shot No. 9

3400 km from ground zero

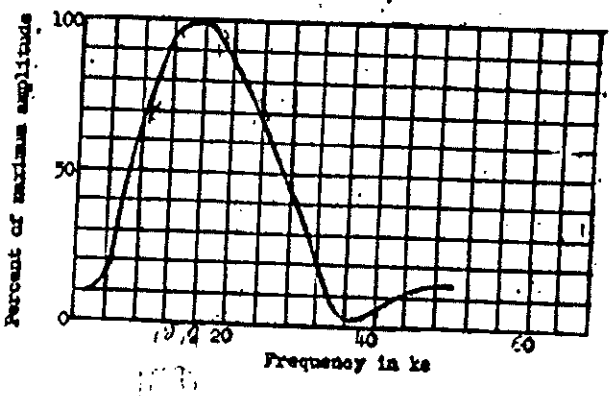

Fig. 3.10c

Frequency function of broad-band pulse

Shot No. 9

3400 km from ground zero

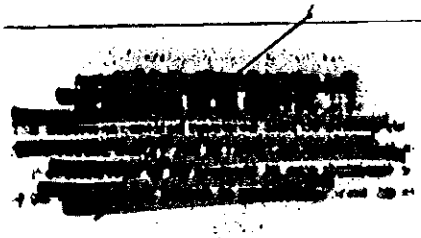

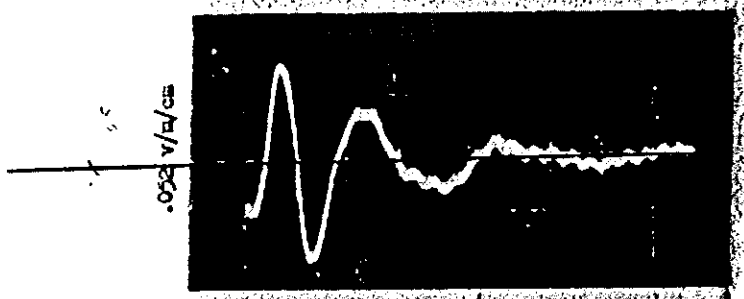

Fig. 3.106

Broadband pulse

Shot No. 10

3400 km from ground zero

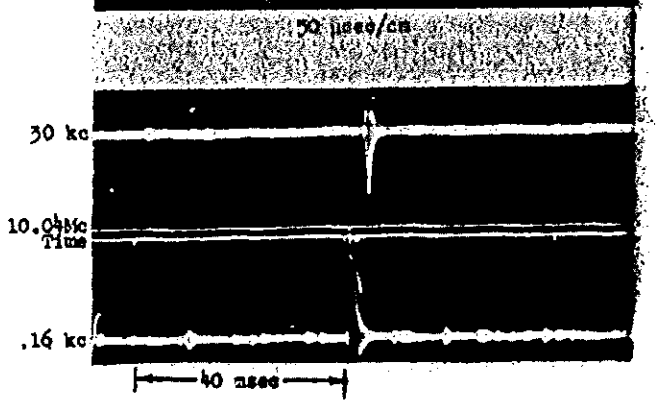

Fig. 3.107

Narrow-band responses

Shot No. 10

3400 km from ground zero

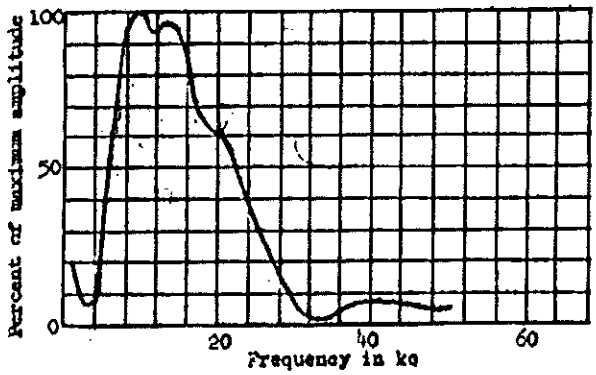

Fig. 3.108

Frequency function of broadband pulse

Shot No. 10

3400 km from ground zero

[redacted]

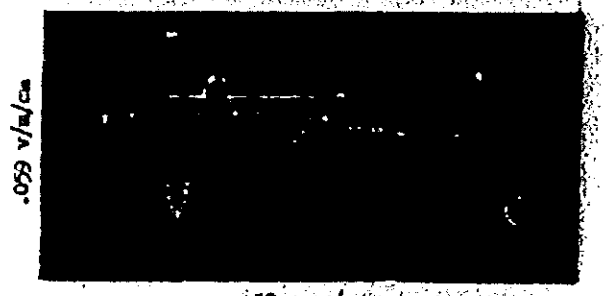

Fig. 3.109

Broadband pulse

Shot No. 11

3400 km from ground zero

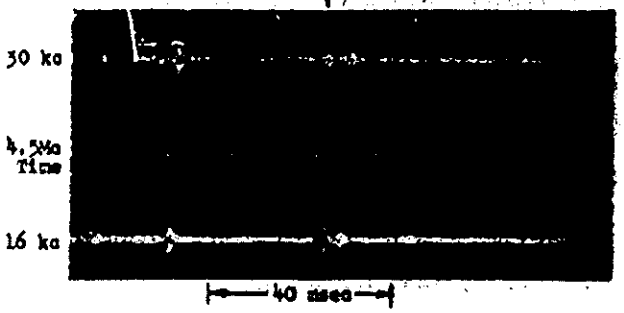

Fig. 3.110

Narrow-band responses

Shot No. 11

3400 km from ground zero

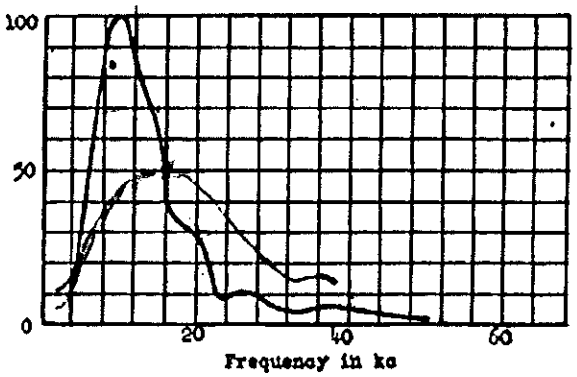

Fig. 3.111

Frequency function of broad-band pulse

Shot No. 11

3400 km from ground zero

[redacted]

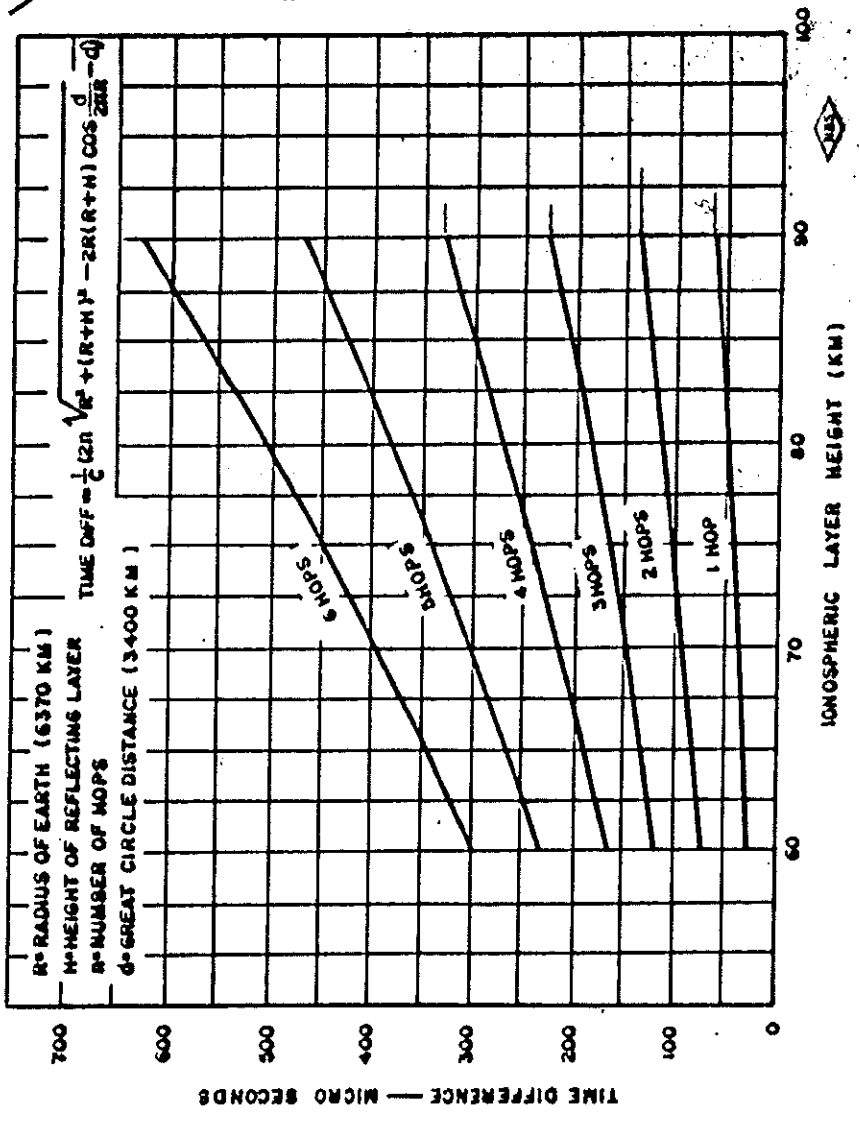

FIG. 3.112 TIME INTERVAL BETWEEN PROPAGATION MODES VS IONOSPHERIC LAYER HEIGHT FOR A 3,400 KM PATH

[redacted]

CHAPTER IV

DISCUSSION OF RESULTS

4.1 ACCURACY OF TIMING AT ALL STATIONS

Measurements of virtual time of detonations were made at all sites, including Stanford. (No discussion of other measurements made at Stanford are given in this report.) Detonation times were computed from the observations at each recording site in accordance with the following

T_o = time of reception of pulse at recording site, using WWV (or WWVH) time as received, uncorrected for propagation delay.
T_s = time of propagation of standard WWV (or WWVH) time signal to recording site.
T_p = time of propagation of pulse signal to recording site.
$T_d = T_o + T_s - T_p$ = astronomical time of detonation.

TABLE 4.1

PARAMETERS FOR COMPUTING ASTRONOMICAL TIME OF DETONATION
(in seconds)

Station	T_s	T_p	$T_s - T_p$
Nevada Proving Ground	0.0115	0.000	0.0115
Boulder	0.008	0.004	0.004
Ft. Belvoir	0.000	0.0115	-0.0115
Stanford	0.014	0.002	0.012

After the approximate detonation times were known, factors such as the relative amplitude of the 15 and 30 kc signals, the time coincidence of pulses recorded on the three narrow-band channels, and the appearance of the broadband waveforms made possible, in most cases, the selection of the correct pulse of each station. When more

[redacted]

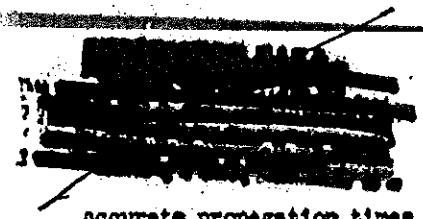

accurate propagation times had been determined, i.e. the delay in arrival of signals from WWV and the actual delay time of the pulse traveling over a known distance, the exact detonation time at Nevada Proving Ground was calculated. The results of such calculations are tabulated in Table 4.2, which shows that all of the detonation times agree to within 3 milliseconds, with one exception.

TABLE 4.2

DETONATION TIMES OBTAINED AT EACH STATION

Shot No.	Date	Nevada	Boulder	Washington	Stanford
1	Mar.17	1320:00.340	1320:00.329	1320:00.341	1320:00.339
2	Mar.24	1310:00.099	1310:00.099	1310:00.100	1310:00.100
3	Mar.31	1300:00.007	1300:00.006	1300:00.009	1300:00.006
4	Apr. 6	1529:38.424	1529:38.424	1529:38.425	1529:38.423
5	Apr.11	1244:59.795	1244:59.791	1244:59.794	1244:59.794
6	Apr.18	1234:59.972	1234:59.970	1234:59.971	1234:59.972
7	Apr.25	1229:59.772	1229:59.773	1229:59.773	1229:59.773
8	May 8	1529:55.374	1529:55.373	1529:55.377	1529:55.375
9	May 19	1204:59.542	1204:59.542	1204:59.543	1204:59.541
10	May 25	1530:00.351	1530:00.348	1530:00.351	1530:00.350
11	June 4	1114:56.692	No record	1114:56.692	1114:56.691

4.2 Discussion of Electromagnetic Radiation and Its Propagation

It is clear from the foregoing that the explosion of an A-bomb gives rise to a pulse of electromagnetic radiation, the principle energy of which lies in the very low frequency part of the radio spectrum with its maximum lying between 15 and 60 kc, for weapons of the sizes used in the UPSHOT-KNOTHOLE tests. It is also clear that the radiation is predominantly plane-polarized with its electric vector perpendicular.

Until a satisfactory model of process has been developed it may be assumed that the radiation is substantially the same as that radiated by shock-exciting a low-frequency, highly-damped antenna. We will assume that this antenna is short as compared with the wavelength at which the energy has a maximum, and that one end is at or close to the surface of the earth.

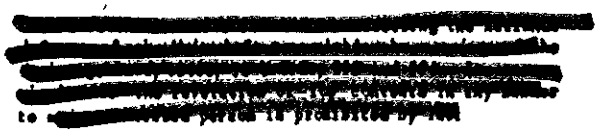

Vertical antennas located at other points on, or close to the surface of the earth, will receive energy from this source by several modes of propagation, each of which has different propagation characteristics. These modes are the surface wave and the several sky waves reflected by the ionosphere. At very great distances, where propagation is achieved by multiple reflections from the ionosphere, the situation is similar to that experienced in wave guides.

4.2.1 Ground-wave Propagation

Energy propagated in the ground wave is attenuated by three principal factors, namely, spreading out of the wave, absorption of the energy by the ground, and diffraction around the earth. This latter factor becomes important at great distances. Over a plane earth the density of energy is given by

$$E = (E_0/d^2)\, e^{-\alpha d} \qquad (1)$$

where E_0 is the energy at unit distance, d, the distance at which the energy is observed, and α, an attenuation index dependent on the electric conductivity and dielectric constant of the ground. Thus at distances close to the source, the inverse distance effect is greater, while at greater distances absorption becomes more important. At distances much over 1000 km the effect of the curvature of the earth becomes important and losses due to diffraction around the earth must be taken into account in addition to the losses mentioned above.

4.2.2 Sky-wave Propagation

Most of the energy radiated from our assumed model is propagated upward through the atmosphere and does not go into the surface wave. Some of this energy is reflected by the ionosphere and returned to the surface of the earth. This is known as one-hop sky-wave propagation. The returned energy may be partially reflected by the earth back to the ionosphere where it may be again reflected and the process repeated any number of times. This is known as multiple-hop sky-wave propagation. Attenuation of the sky-wave modes is determined by the spreading out of the wave and by losses through reflection at the ionosphere and at the earth. The energy density at some distance d, due to each mode is given by

$$E = (E_o/d^2)\, R_i^n\, R_e^{n-1} \qquad (2)$$

in which E_o is the energy density at unit distance from the source in the direction of the central ray for that particular mode, R_i and R_e, the reflection coefficients of the ionosphere and the earth, and n, the number of hops in the mode. In most cases R_e is considerably greater than R_i and may be considered unity.

The value which R_i may assume covers a wide range. It depends on geographic location, time of day, season of year, azimuth of propagation, and angle of incidence on the ionosphere. For small angles of incidence, i.e. when the energy is propagated nearly normal to the ionosphere, R_i is small, 0.01 or less, but at larger angles, particularly at night, it may approach unity. Because of the smallness of R_i for small angles of incidence, only the modes having a few reflections at rather large angles deliver much energy at a distant point, and sky-wave modes are of little importance at short distances for low-frequency propagation. The angles of incidence are calculated on the basis of classical geometric optics, regarding the ionosphere and the earth as two concentric spherical mirrors, concave and convex, separated by a distance of 70 to 90 km for low-frequency waves.

Because of differences in length of path traversed by the ground wave and the several sky-wave modes from the source to a receiving point, the waves arriving by one mode may be in or out of phase with respect to another at certain frequencies. This gives rise to regions where the signal is enhanced or diminished with respect to what it would be if only one mode were active. However, if a transmitted signal consists of a pulse representable by a band of frequencies, and the difference in travel time by different modes is such that the signals from two or more modes merge, an alteration in the form of the received pulse occurs. This results in a change in the spectral representation of the pulse, some frequency regions being enhanced and other diminished. It is not possible that enhancement or diminution can occur throughout the spectral range of the pulse.

[redacted]

[redacted]

4.2.3 Wave-guide Concepts

At distances from the source sufficiently great that a number of independent, large angle, sky-wave modes can be active, the energy radiated at low angles from the source may be regarded as trapped between the earth and the ionosphere. In this case it is convenient to consider propagation as a wave-guide phenomenon. The energy is attenuated by spreading out of the wave, but in this case, since the energy does not spread out in three dimensions, it is attenuated proportionately, approximately to the inverse first power of the distance instead of the inverse square. Additional attenuation results from absorption in the wave guide. The energy density at any point at distance d may be given by

$$E = E_1(d_1/d)\left(\frac{\sin \theta_1}{\theta_1}\right)\left(\frac{\theta}{\sin \theta}\right) e^{-\alpha(d-d_1)} \qquad (3)$$

in which E_1 is the energy density at distance d_1 where one may begin to apply the wave guide concept, and θ and θ_1 are the angular measures of d and d_1 to correct for the finite curvature of the earth. The index, α, is the absorption coefficient of the wave guide. The equation may be expressed in more usable form

$$E = K(E_0/d)\left(\frac{\theta}{\sin \theta}\right) e^{-\alpha d} \qquad (4)$$

in which K is a coefficient of coupling in launching the wave-guide mode and E_0 has the same significance as in Equation (1), but α does not have the same value as in Equation (1).

4.2.4 Applications to Observations Reported

We may now consider the application of these principles to the measurements described in this report. The Nevada Proving Ground sites are well within the region where practically all the energy received is transmitted from the source by the ground-wave mode. Because of the closeness of the receiving site to the source, in all cases, and the low attenuation by ground absorption for the spectrum range of the pulse, the shape of the pulse, as received at these sites, is but little altered by propagation effects.

[redacted]

[redacted]

[redacted]

Ft. Belvoir is well within the region where the waveguide model may be considered applicable. At this distance the ground wave is so strongly attenuated by ground absorption and losses due to diffraction around the earth that it may be considered completely absent. The one-hop sky-wave mode delivers no appreciable energy because a direct one-hop path is not geometrically possible, so that energy to excite this mode must be diffracted around the earth with attendant heavy losses. Two-, three-, four- and higher-hop modes are permissible, and the angles of incidence are so great that the reflection coefficients are large.

The site at Boulder lies in a transition region. The ground wave and the one-hop sky wave deliver nearly all the energy. Higher order modes are also active, but except for the two-hop mode, little energy is delivered by them because of the low reflection coefficients for the small angles of incidence involved. It is convenient to assume that Boulder is at a sufficient distance from the Nevada Proving Ground that wave-guide approximations may be considered from that point outward.

4.3 EVALUATION OF PROPAGATION CONSTANTS

Various constants used for calculation of field strengths at low frequencies appear in the literature. However, because of the very special nature of these observations, it was considered desirable to derive new constants from the data themselves.

The first step was to calculate the total energy density recorded at each of the sites. This was done by measuring the deflections of the oscilloscopes caused by the pulse at regular intervals of time, Δt. The ordinates so obtained were squared and multiplied by the square of the reduction factor for conversion of oscilloscope deflection to volts per meter and by the length of the time interval involved. The quantities so obtained were summed and divided by 377 ohms to give the results in joules per square meter. The procedure is represented in the following equation.

$$E = h^2 v^2 \Delta t / 377 \text{ ohms} \qquad (5)$$

in which h^2 is the ordinate in centimeters on the oscilloscope, v the reduction factor, and Δt the time interval between ordinates.

[redacted]

[redacted]

[redacted]

In addition the energy values obtained from the observations at the Nevada Proving Ground were normalized to a distance of 1 km from the source in accordance with Equation (1). This was done so that energy from the various shots could be compared since the distances of the recording sites from the source were different for the various shots. In making this normalization it was assumed that ground-wave absorption over such short distances was negligible.

The energy densities calculated for the various shots are presented in Table 4.3. In cases where data are lacking in the table, suitable records for calculating the energy were not obtained. Also the energy values for Shots No. 6, 7, and 8 at Ft. Belvoir are a little too low, due to the filter which was connected in the receiving circuit to eliminate interference from NSS.

TABLE 4.3

ELECTROMAGNETIC ENERGY RADIATED FROM SHOTS NO. 2 - 11

Shot No.	Total Energy E_T (Joules)	Energy Density E_0 Observed at NPG Normalized to 1 km (J/m^2)	Energy Density E_1 Observed at Boulder (J/m^2)	Energy Density E_2 Observed at Ft. Belvoir (J/m^2)
2	8.1×10^6	1930×10^{-3}	$.299 \times 10^{-6}$	
3	0.22×10^6	53×10^{-3}		
4	0.51×10^6	121×10^{-3}		
5	0.12×10^6	28×10^{-3}		
6	10.4×10^6	2490×10^{-3}	175×10^{-6}	$.018 \times 10^{-6}$
7	15.9×10^6	3800×10^{-3}	$.185 \times 10^{-6}$	$.023 \times 10^{-6}$
8	5.7×10^6	1360×10^{-3}	107×10^{-6}	$.009 \times 10^{-6}$
9	10.4×10^6	2480×10^{-3}	158×10^{-6}	$.007 \times 10^{-6}$
10	2.8×10^6	680×10^{-3}	041×10^{-6}	$.004 \times 10^{-6}$
11	9.2×10^6	2200×10^{-3}		$.009 \times 10^{-6}$

[redacted]

[redacted] SECRET

Examination of the pulses recorded at Boulder suggests that the first part of the pulse is due to arrival of the surface wave and that the one-hop sky wave arrives just as the surface wave has almost completely passed. If this is true about half the energy is delivered by the surface wave and half by the one-hop sky wave. We may then calculate the ground-wave attenuation from data in Table 4.3. For convenience we may express Equation (1) in logarithms to the base 10.

$$\log E = \log E_0 - 2 \log d - k_g d \qquad (6)$$

Values of $k_g d$ and of k_g, expressed in decibels per 1000 km, are given in Table 4.4. The value of k_g is relatively great, corresponding to ground of very poor conductivity, $\sigma \leq 10^{-15}$ emu. It also includes effects due to diffraction losses. The reflection coefficient for the ionosphere, for the time of day at which each observation was made, at the angle of incidence involved in the one-hop mode may be calculated from Equation (2). These results are also shown in Table 4.4. E_0 was taken to be equivalent to E_0 of the surface wave. The reflection coefficients in the table are ratios of energy in the incident and reflected waves, not field strengths. If they represented field strengths the values would range from 0.16 to 0.20 which are not inconsistent with values commonly given in the literature.

TABLE 4.4

GROUND ATTENUATION INDEX AND IONOSPHERIC REFLECTION COEFFICIENTS FOR DISTANCE OF 1000 KM

Shot No.	$k_g d$ ($\log_{10}$)	k_g (db/100 km)	R_1
6	1.64	16	0.023
7	1.62	16	0.024
8	1.40	14	0.040
9	1.50	15	0.032
10	1.52	15	0.030
Average	1.50	15	0.030

[redacted]

TABLE 4.3

ATTENUATION INDEX AND "COUPLING COEFFICIENTS" FOR WAVE GUIDE MODEL BEYOND 1000 KM

Shot No.	K		k_g
	($\log_{10}$)	antilog	(db/1000 km)
6	6.02 - 10	10.5×10^{-5}	1.9
7	5.83 - 10	6.8×10^{-5}	1.5
8	6.13 - 10	13.5×10^{-5}	2.3
9	6.13 - 10	13.5×10^{-5}	3.3
10	5.98 - 10	9.6×10^{-5}	2.0
Average	6.02 - 10	10.8×10^{-5}	2.2

The constants for the wave-guide model of propagation to great distances may be derived from the values of energy densities given in Table 4.3. Expressing Equation (4) in logarithms to the base 10 and neglecting the term $\theta/\sin\theta$, which is substantially unity, we have

$$\log E_y = \log K + \log E_0 - \log d - k_g d \qquad (7)$$

There are two parameters to be determined, K and k_g. Using the data from Nevada Proving Ground, Boulder, and Ft. Belvoir, the calculated parameters are as given in Table 4.3. It is interesting to calculate from these parameters the energy to be expected at Ft. Belvoir for Shot No. 11, for which no observations are available at Boulder. The calculated value is 0.0120×10^{-6} joules per square meter, and the observed value was 0.00947×10^{-6} joules per square meter.

In spite of the relatively good agreement of the constants determined from the individual shots, some reservations must be made in applying them for propagation calculations under other conditions. The ground attenuation index k_g is accurately determined for the particular terrain involved, but over regions of good conductivity it would be considerably less. For propagation over sea water,

absorption effects are negligible, the principal loss in the surface wave, apart from inverse distance squared, being due to diffraction which is important at distances over several hundred kilometers.

The reflection coefficient of the ionosphere as given in Table 4.4 is reliable for calculation of received energy for approximately equal distances and similar zenith angles of the sun. The value is not suitable for use when the path lies in darkness.

The coupling coefficient and attenuation index calculated for the wave-guide model are subject to some uncertainty since observations at only two distances, 1000 km and 3400 km, were used in the calculations. The small value of the effective coupling coefficient is due in part to the arbitrary determination to use the energy at unit distance (in this case taken as 1 km) as a reference value. This accounts for about a hundred-fold reduction in the apparent coupling coefficient, the remaining factor of 100 resulting from escape of the energy from the earth-ionosphere boundaries within the first few hundred kilometers. Expressed in decibels, there is a 40 db loss represented by the effective coupling coefficient, 20 db of which arises from geometric considerations inherent in the assumption regarding the point where E_0 is measured, and the remaining 20 db from actual leakage.

A different distribution of losses between the coupling coefficient and the attenuation index might have resulted if observations had been made at other distances than those given, and certainly if the source and receiving sites had all been in darkness. However, the attenuation index is not likely to be in appreciable error for daylight propagation. Furthermore, it is in good agreement with the attenuation index for daylight propagation in the very low frequency range as obtained from numerous measurements made on continuous-wave transmitters operating at very low frequencies.

4.4 ENERGY RADIATED FROM SOURCE

The energy densities calculated from the observations at the sites at Nevada Proving Ground may be used to derive the total electromagnetic energy radiated by each bomb. Assuming again that radiation occurred from a short vertical dipole, the energy radiated in any direction is proportional to $\cos^2\theta$, where θ is the angle of elevation above the horizontal. The total energy radiated is given by

$$E_T = E_0 d^2 \int_0^{2\pi} \int_0^{2\pi} \cos^2\theta \, d\phi \, d\theta = 4\pi E_0 d^2 / 3 \qquad (8)$$

in which E_0 is the energy density at a point at the earth's surface distance d from the source, and ϕ is the azimuth of the observing point from the source. Values of E_T in joules are given in Table 4.3.

The energy values range from 0.119×10^6 to 15.9×10^6 joules. By comparison, the electromagnetic energy in the frequency range from 7.5 kc to 10 kc radiated from lightning flashes averages around 0.2×10^6 joules.[3] Since the pulse emitted has a duration of only about 50 microseconds, these values correspond to an average radiated power for the duration of the pulse of from 2,400 to 300,000 megawatts.

For the sizes of the weapons fired during the tests under discussion, a fairly good linear relationship between the total electromagnetic energy radiated and the bomb yield obtains. A plot of this relationship appears in Figure 4.1, where total energy is plotted against yield in kilotons. For convenience the energy density, normalized to one kilometer from ground zero, is shown as an additional abscissa scale. In drawing the line on the graph Shots No. 4, 8, 10 and 11 were ignored since they were not tower shots.

All of the air-dropped bombs and the cannon-launched bomb showed conspicuously less electromagnetic radiation for the same yield than those fired on the towers. An empirical relationship to correct for the effect of height was derived and applied to the values for the non-tower shots to give the equivalent radiated energy to be expected if the shots had been fired on towers. A new plot, with the correction applied to the non-tower shots, is shown in Figure 4.2. All except Shot No. 8 show close agreement in the relationship between yield and radiated energy. The equation relating energy to yield is

$$E_T = 0.362\, Y / (1+h) \qquad (9)$$

where E_T is the electromagnetic energy radiated in megajoules, Y the yield in kilotons, and h the height of detonation in thousands of feet above ground, a correction to be applied only for non-tower shots. The energy density at a distance of one kilometer is given by

[redacted]

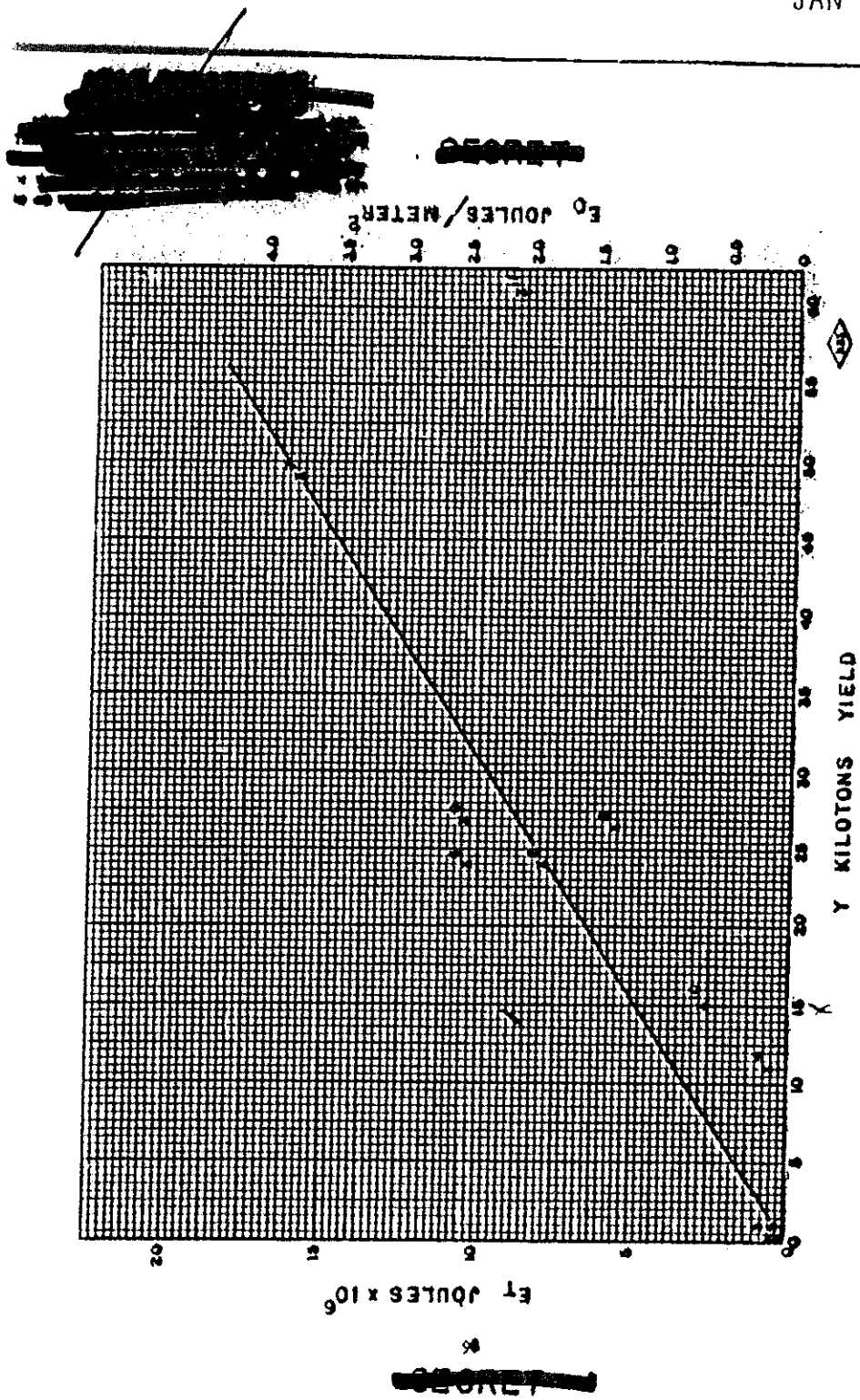

FIG. 4-1 RADIATED ENERGY AS A FUNCTION OF YIELD

FIG. 4.2 RADIATED ENERGY AS A FUNCTION OF YIELD (APPLYING CORRECTION FOR HEIGHT)

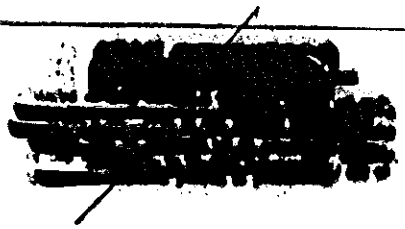

$$E_0 = 0.086\ Y / (1+h) \qquad (10)$$

E_0 , in this case being in joules per square meter.

Some reservations must be held regarding the reliability of the absolute values of the energies calculated from the data obtained at the Nevada Proving Ground, although the relative values are undoubtedly reliable. The small value for the coupling coefficient and the high value for absorption of the ground wave as received at Boulder, calculated previously, suggest that the energies may be too large.

The linear relationship between yield and total radiated energy, when the height corrections are applied, may be fortuitous. Nothing can be concluded regarding their applicability to weapons having yields far outside the ranges of those involved here, or to other types such as thermonuclear weapons.

4.5 DIRECTION OF THE ELECTRIC VECTOR OF THE RADIATED FIELD

Considerable interest is attached to the direction of the electric vector radiated from the source and recorded at the near receiving sites. The direction of this vector for the main initial phase of the pulse was the same in all cases.

To obtain the relation between the direction of current flow in the source, and the direction of deflection of the oscilloscope, we express the radiation electromagnetic field in terms of the vector potential $\underline{A}$, and then relate the latter to the source current $\underline{i}$:

$$\underline{E} = -\frac{\partial \underline{A}}{\partial t} \; ; \qquad \underline{H} = \nabla \times \underline{A}$$

$$\underline{A}(\underline{r}', t) = \int_V \frac{\underline{i}(\underline{r}, t - \frac{r}{a})}{|\underline{r} - \underline{r}'|} \, dv$$

Thus a current which is increasing in the downward direction gives rise to an electric field positive in the upward direction. This conclusion may be checked through $\underline{H}$, using the fact that the Poynting vector $\underline{E} \times \underline{H}$ is positive in the direction of energy flow.

The antenna-oscilloscope connections were such that a negative deflection corresponded to an electric field positive upward at the receiving site. We therefore conclude that the main current in the source was increasing downward initially for all cases. This does not apply to the small positive-going precursors observed in some cases.

REFERENCES

1. Ronald King and F. G. Blake, Jr., "The Self-Impedance of a Symmetrical Antenna", Proc. IRE, July, 1942, Vol. 30, p. 339

2. Frederick Emmons Terman, Radio Engineers Handbook (McGraw-Hill Book Company, 1943), First Edition, p. 813

3. K. G. Jansky, "An Experimental Investigation of the Characteristics of Certain Types of Noise", Proc. IRE, 1939, Vol. 27, pp. 763-768.

4. R. D. England and R. E. Partridge, Jr., "Investigation of Early Electromagnetic Signals", Los Alamos Scientific Laboratory, University of California, Nov. 1953.

5. T. H. Laby, J. J. McNeill, F. G. Nicholls and A. F. B. Nickson, "Waveform Energy and Reflection by the Ionosphere of Atmospherics", Proc. Roy. Soc., 1940, 174, pp. 145-163.

6. J. D. Best, J. A. Ratcliffe, and M. V. Wilkes, "Experimental Investigations with Very Long Waves Reflected from the Ionosphere", Proc. Roy. Soc., Sept. 1936, 156, p. 614.

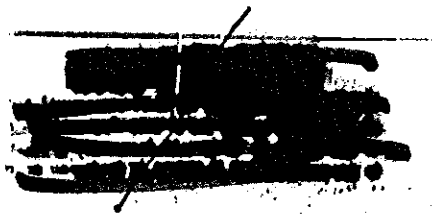

SECRET

SECRET

[redacted]

[redacted]

THE NATIONAL BUREAU OF STANDARDS [redacted]

Functions and Activities

The functions of the National Bureau of Standards are set forth in the Act of Congress, March 3, 1901, as amended by Congress in Public Law 619, 1950. These include the development and maintenance of the national standards of measurement and the provision of means and methods for making measurements consistent with these standards; the determination of physical constants and properties of materials; the development of methods and instruments for testing materials, devices, and structures; advisory services to Government Agencies on scientific and technical problems; invention and development of devices to serve special needs of the Government; and the development of standard practices, codes, and specifications. The work includes basic and applied research, development, engineering, instrumentation, testing, evaluation, calibration services, and various consultation and information services. A major portion of the Bureau's work is performed for other Government Agencies, particularly the Department of Defense and the Atomic Energy Commission. The scope of activities is suggested by the listing of divisions and sections on the inside of the front cover.

Reports and Publications

The results of the Bureau's work take the form of either actual equipment and devices or published papers and reports. Reports are issued to the sponsoring agency of a particular project or program. Published papers appear either in the Bureau's own series of publications or in the journals of professional and scientific societies. The Bureau itself publishes three monthly periodicals, available from the Government Printing Office: The Journal of Research, which presents complete papers reporting technical investigations; the Technical News Bulletin, which presents summary and preliminary reports on work in progress; and Basic Radio Propagation Predictions, which provides data for determining the best frequencies to use for radio communications throughout the world. There are also five series of nonperiodical publications: The Applied Mathematics Series, Circulars, Handbooks, Building Materials and Structures Reports, and Miscellaneous Publications.

Information on the Bureau's publications can be found in NBS Circular 460, Publications of the National Bureau of Standards ($1.25) and its Supplement ($0.75), available from the Superintendent of Documents, Government Printing Office. Inquiries regarding the Bureau's reports and publications should be addressed to the Office of Scientific Publications, National Bureau of Standards, Washington 25, D. C.

[redacted]

NBS

DEPARTMENT OF DEFENSE
WASHINGTON HEADQUARTERS SERVICES
1155 DEFENSE PENTAGON
WASHINGTON, DC 20301-1155

[redacted]

28 JAN 2013

Subject: OSD MDR Case 12-M-1573

Dear [redacted],

We have reviewed the enclosed document in consultation with the Department of Energy (DOE) and have declassified it in part. OSD excised information is exempt from declassification under Executive Order 13526, section 6.2(a) and is also protected under the Freedom of Information Act (FOIA), 5 U.S.C. § 552(b)(6). DOE excised information is exempt from declassification under section 6.2(a). Section 6.2(a) protects "Restricted Data" and "Formerly Restricted Data" information in conformity with the provisions of the Atomic Energy Act of 1954, as amended, and regulations issued under that Act. FOIA, 5 U.S.C. § 552(b)(6) protects information which would constitute a clearly unwarranted invasion of the personal privacy of certain individuals.

OSD stands as the appellate authority and will coordinate any appeals regarding this case. A written appeal must be filed within 60 days explaining the rationale for reversal of the decision. Reference should be made to OSD MDR Case 12-M-1573. Letters of appeal should be sent to the following address:

WHS/ESD Records and Declassification Division
Attention: Robert Storer
4800 Mark Center Drive
Suite 02F09-02
Alexandria, VA 22350-3100

If you have any questions, contact me by e-mail at Records.Declassification@whs.mil or by phone at 571-372-0483.

Sincerely,

Robert Storer

Robert Storer
Chief, Records and Declassification Division

Enclosures:
1. MDR request
2. Document 1

DEPARTMENT OF DEFENSE
WASHINGTON HEADQUARTERS SERVICES
1155 DEFENSE PENTAGON
WASHINGTON, DC 20301-1155

FEB 14 2013

MEMORANDUM FOR DEFENSE TECHNICAL INFORMATION CENTER
(ATTN: DTIC-OQ INFORMATION SECURITY)
8725 JOHN J. KINGMAN ROAD, STE 0944
FT. BELVIOR, VA 22060-6218

SUBJECT: OSD MDR Cases 12-M-1572 and 12-M-1573

At the request of [redacted], we have conducted a Mandatory Declassification Review of the attached documents under the provisions of Executive Order 13526, section 3.5, for public release. We have declassified the documents in part. We have attached a copy of our response to the requester on the attached Compact Disc (CD). If you have any questions, contact me by e-mail at storer.robert@whs.mil, robert.storer@whs.smil.mil, or robert.storer@osdj.ic.gov or by phone at 571-372-0483.

Robert Storer

Robert Storer
Chief, Records and Declassification Division

Attachment:
CD